SOX2 is required independently in both stem and differentiated cells for pituitary tumour genesis in *p27* null mice.

Veronica Moncho-Amor[1], Probir Chakravarty[2], Christophe Galichet[1], Ander Matheu[3], Robin Lovell-Badge[1*] and Karine Rizzoti[1*].

1 Laboratory of Stem Cell Biology and Developmental Genetics, The Francis Crick Institute, 1 Midland Road, London NW1 1AT, UK
2 Bioinformatics core, The Francis Crick Institute, 1 Midland Road, London NW1 1AT, UK
3 Cellular Oncology Group, Biodonostia Health Research Institute, San Sebastian, Spain; CIBER de Fragilidad y Envejecimiento Saludable (CIBERfes), Madrid, Spain; IKERBASQUE, Basque Foundation, Bilbao, Spain.
* authors for correspondance robin.lovellbadge@crick.ac.uk and karine.rizzoti@crick.ac.uk

Abstract

Loss of the pleiotropic protein P27 predominantly results in development of pituitary intermediate lobe (IL) tumours in mice. In humans, P27 levels are reduced in many cancers, and inactivating mutations cause Multiple Endocrine Neoplasia type 4 (MEN4) syndrome. We previously showed that P27 can drive repression of the transcription factor *Sox2*. This interaction plays an important role during development of *p27-/-* IL tumours because loss of one copy of *Sox2* diminishes tumorigenesis. Here, we have explored the cellular origin and mechanisms underlying melanotroph tumorigenesis in *p27-/-* IL, and the role of SOX2 in this process. It was found that IL hyperplasia is associated with reduced cellular differentiation, while levels of SOX2 are substantially increased in both stem cells (SC) and melanotrophs. Using conditional loss-of-function and lineage tracing approaches, we show that SOX2 is required cell-autonomously in *p27-/-* melanotrophs for these to give rise to tumours, and also in SCs for these to promote tumour growth. This is supported by studies deleting the *Sox2* regulatory region 2 *(Srr2)*, which is the target of P27 repressive action. Single cell transcriptomic analysis of IL reveals that activation of a SOX2-dependent MAPK pathway in SCs is important for tumorigenesis. Altogether, our data highlight different aspects of the role of SOX2 following loss of *p27,* according to the cellular context. Furthermore, we uncover an unexpected SOX2-dependent paracrine function for SCs, which promotes alteration of melanotroph identity and tumour formation. In conclusion, our results imply that targeting SCs, in addition to tumour cells themselves, may represent an efficient anti-tumoral strategy in certain contexts.

Introduction

Tumour formation involves a complex interplay of cellular interactions. Most frequently, transformed cells interact with their microenvironment, which provides a supportive niche for the formation, maintenance and dissemination of the tumour [1]. In addition, the tumours often display considerable cellular heterogeneity, which can include the presence of cancer stem cells (CSCs). These are a subpopulation of undifferentiated tumoral cells that may originate from resident tissue stem cells (SCs), and which fuel growth and recurrence of the tumour [2]. In rarer cases, cells acquiring mutations may not form the tumour themselves, but instead induce others to do so. This has been observed in the murine intestine [3], liver [4], skin [5], in leukaemia [6], and in the pituitary where tissue SCs harbouring a Wnt pathway activating mutation recruit surrounding cells to form tumours resembling human craniopharyngiomas [7].

The pituitary is a small endocrine gland located just under the brain, connected to the hypothalamus that controls its secretions. In the mouse it comprises three lobes, the posterior lobe, comprising axon terminals and glial cells, the anterior lobe (AL), which is highly vascularized and contains most endocrine cell populations, and the intermediate lobe (IL), which is avascular [8] and populated by a single endocrine population; these are melanotrophs that secrete melanocyte stimulating hormone (MSH). MSH is processed from its precursor pro-opio-melanocortin (POMC), which is also produced in AL by corticotrophs, where it is cleaved into adrenocorticotropic hormone (ACTH) [9]. Expression of *Pomc* is controlled in both cell types by the T-box factor TBX19 [10]. In the embryo, the pioneer transcription factor PAX7 controls acquisition of the melanotroph versus corticotroph fate [11]. Melanotrophs are quiescent [12], in contrast with AL endocrine cells, however, they are particularly sensitive to mutations affecting cell cycle regulators [13]. In mice deleted for *p27*, encoding a protein best known for its negative cell cycle regulatory role [14], IL tumorigenesis in mature animals is the hallmark of pleiotropic effects [15,16,17]. In humans, *P27* mutations impairing protein function cause multiple endocrine neoplasia syndrome, MEN4, and low levels of P27 in tumours are generally associated with a poor prognosis [18]. In the developing pituitary, P27, along with P57, is necessary for cell cycle exit in differentiating endocrine cells [19]. However, its is not limited to cell cycle regulation, because in *Cyclin D1*$^{-/-}$*; p27*$^{-/-}$ compound mutants, pituitary hyperplasia is still present [20].

We have previously demonstrated that P27 can recruit co-repressors to regulate gene expression. More precisely, P27 can repress the expression of the transcription factor SOX2 during differentiation of induced pluripotent SC (iPSC) [21]. SOX2 is essential during embryonic development, for maintenance of adult SC properties in different cell lineages, and for somatic cell reprogramming [22]. Its expression is elevated in many cancers and this is associated with increased proliferation, invasiveness, lineage plasticity, chemoresistance and, in consequence, poor prognosis [23,24,25]. *In vivo*, the SOX2-P27 interaction is particularly relevant for IL because deletion of one copy of *Sox2* diminishes tumorigenesis in *p27*$^{-/-}$ animals [21].

SOX2 is expressed in melanotrophs where it is required embryonically for expression of PAX7 [26]. In addition, SOX2 is expressed in a population of adult pituitary SCs [7,27,28]. Interestingly, in *p27*$^{-/-}$ mice, the thickness of the SOX2^{+ve} SC layer is increased [21]. Therefore, while the importance of the SOX2-P27 interaction for IL tumorigenesis is apparent, the modalities of this interaction and, in particular, the roles of SOX2 in the SCs and melanotrophs required for this are unknown.

In this study, we have examined how IL tumorigenesis develops in *p27*$^{-/-}$ mice, and explored the role of SOX2 in this process. As *p27*$^{-/-}$ IL become hyperplastic, melanotrophs tend to lose differentiated features and display increased levels of SOX2 expression, which is also observed in SCs. To

determine the cellular origin of the tumors, and explore SOX2 function independently in melanotropsh and SCs, we have performed lineage tracing experiments and deleted of the gene conditionally. Our results demonstrate that SOX2 is required independently in *p27*$^{-/-}$ melanotrophs and SCs for tumorigenesis. Analyses of deletion of the *Sox2* regulatory region 2 *(Srr2)*, which is the target of P27 repressive action, supports the pro-tumorigenic role of SOX2 in SCs. Finally, single cell transcriptomic analyses of IL reveals that activation of a SOX2-dependent MAPK pathway in SCs is important for tumorigenesis. In conclusion, our study emphasizes the pleiotropic effects of SOX2 in *p27*$^{-/-}$ IL and uncovers an unexpected paracrine role for SCs in IL tumour formation, suggesting that these, or the relevant signaling molecules, represent good anti-tumoral targets, in addition to tumour cells themselves.

Results

Characterization of intermediate lobe tumours in *p27-/-* pituitaries.

We first examined P27 by immunofluorescence and observe widespread nuclear expression throughout the anterior pituitary with varying levels of expression (Fig1A), in agreement with fluctuations of P27 according to the cell cycle [29]. Anterior endocrine and stem cells proliferate rarely [30, 27] and P27 levels are relatively high in these. However, even though IL melanotrophs have been shown to be quiescent [12], P27 immunostaining is much weaker compared with the AL and SCs. We then examined SOX2, which is expressed both in SCs [27], and, at lower levels, in melanotrophs [26] (Fig1A). In wild-type animals, P27 and SOX2 proteins are clearly co-expressed. In *p27-/-* pituitaries, the SC layer appears thicker in mutants [21]. In agreement with a repressive action of P27 on *Sox2* expression [21], SOX2/*Sox2* levels are significantly up-regulated both in SCs and melanotrophs in *p27-/-* pituitaries (Fig1A-C).

To further characterize initiation and development of the tumours in *p27-/-* mice, we performed transcriptomic analyses from dissected IL (Fig1D-F Supplementary Fig1A). Before tumour formation, at two months of age, we detected 249 differentially expressed genes (DEG) between *p27-/-* and control samples. In seven-month old animals, when hyperplasia is very clear, there are 3736 DEG. At both stages, upregulation of cell cycle markers is observed, in agreement with the CDKI function of P27. Both datasets also suggest a reduced activity of Notch signalling in mutants, with reduced expression of *Notch1* and *2* receptors and the target *Hey1*, which are all normally expressed in SCs [31,32]. Furthermore, transcript levels for several members of the Hippo pathway are affected. Both Notch and Hippo pathway dysregulation have been associated with tumour development [33 34]. We also observe downregulation of genes associated with the cytoskeleton and cell adhesion which may reflect disruption of the direct interaction between P27 and RhoA [35]. Furthermore, downregulation of POMC and genes associated with its processing suggests an alteration of melanotroph function and/or identity in mutants.

We further investigated whether melanotroph function and/or identity have been altered, something that has not been reported previously [15,16,17]. We observe a significant downregulation of POMC/*Pomc* expression levels, exclusively in *p27-/-* melanotrophs post-natally, but prior to tumour formation (Fig1G-H), while corticotrophs appear unaffected. In agreement with these data, radio-immunoassays [36] show that levels of MSH are reduced while ACTH is unaffected in *p27-/-* pituitaries (Fig1H). *p27-/-* mice are affected by gigantism, which has been attributed to general loss of cell cycle repression [15,16,17], however, an additional explanation could be the significant increase in pituitary GH content we observe (Supplementary Fig1B). This shows that the anterior pituitary is affected by loss of *p27*. TBX19 is a direct upstream regulator required for *Pomc* expression [37]. In agreement with a reduction in *Pomc* levels, *Tbx19* levels are significantly reduced in IL, while *Pax7* [11] also appear reduced, although not to a statistically significant degree (Fig1I). Moreover, *p27-/-* melanotrophs are smaller than those in wild-type pituitaries (Fig1J). Altogether, these results suggest that melanotroph identity and/or post-natal maturation are altered in *p27-/-* mutants, and this occurs before tumours develop.

We then examined cell proliferation by quantifying incorporation of EdU in IL, dorsal (flanking IL), and ventral SC layer (flanking AL) (Fig1K-N). In E18.5 embryos, proliferation tends to increase in both IL and its flanking SC layer in the mutants, however, this is not statistically significant (Fig1K). In contrast, in one-month old mutant animals, we observe a significant increase in proliferation of both melanotrophs and adjacent SCs (Fig1L-N). In seven-month old animals, increased proliferation

is observed in all compartments of the mutants compared to controls, in agreement with the transcriptomic analysis results (Fig1E,F). To further test the proliferative capacity of SCs, we performed pituisphere assays [27] separately from anterior and intermediate lobe cells and observed an increased sphere forming ability from *p27*$^{-/-}$ IL cells (Fig1O). Altogether these results suggest that, while both SC layers behave abnormally in *p27*$^{-/-}$ pituitaries, the SCs in direct contact with melanotrophs are more affected, suggesting that there may be some non-cell autonomous consequences to the loss of *p27*.

HIF-1 activation is associated with tumour angiogenesis and its targets are up-regulated in seven-month old *p27*$^{-/-}$ IL transcriptomes (Fig1E). Moreover, *p27*$^{-/-}$ IL tumours are haemorrhagic [15]. We thus examined CD31 expression and observe development of ectopic blood vessels in juvenile *p27*$^{-/-}$ IL, coincident with the abnormal increase in rates of cell proliferation (Fig1P).

In conclusion, *p27* deletion results in increased cell proliferation and ectopic vascularization, and with altered activity of several signalling pathways, including those involving Notch and Hippo. While P27 protein is already present at higher levels in the embryo [19], these defects appear to only become significant post-natally, in both melanotrophs and SCs. In addition, melanotroph identity and/or maturation appears affected in mutants.

Characterization of the SOX2-P27 interaction in *p27*$^{-/-}$ mutants.

Deletion of one copy of *Sox2* is sufficient to dramatically reduce occurrence of IL tumours (Fig2A, C) [21], however, hyperplasia is still observed in *p27*$^{-/-}$*;Sox2*$^{+/-}$ IL (Fig2A). We further characterized the SOX2-P27 interaction by demonstrating that survival of *p27*$^{-/-}$ mutants (12.5 months, n=28) was significantly improved by *Sox2* haploinsufficiency (17.1 months, n=10) (Fig2B). However, in agreement with cell type specificity for the SOX2-P27 interaction, while pituitary and duodenum tumours were sensitive to *Sox2* dosage, lung tumour development was unaffected (Fig2C).

We then performed comparisons of the transcriptomes of wild-type, *p27*$^{-/-}$ and *p27*$^{-/-}$*;Sox2*$^{+/-}$ IL (Fig2D, Supplementary Fig2A). To pinpoint genes underlying IL tumour impairment in compound mutants, and conversely those associated with higher levels of SOX2 and tumorigenesis, we focused our analyses on those that were exclusively differentially expressed in *p27*$^{-/-}$, and therefore restored to control levels in *p27*$^{-/-}$*;Sox2*$^{+/-}$ samples. We obtained a list of DEG and pathways comparable to our previous analysis (Fig1D, Fig2D). This suggests that SOX2 is not required for a specific aspect of tumour formation in *p27*$^{-/-}$ mice, but rather that it has a broad and therefore probably early role in tumour genesis. Reduced *Sox2* dosage is associated with a decrease in proliferation and HIF1-target gene expression, in agreement with less angiogenesis linked with reduced overproliferation in *p27*$^{-/-}$*;Sox2*$^{+/-}$ mutants. We also observed an effect on genes involved in cytoskeleton, suggesting that reduction of *Sox2* allows restoration of a cellular phenotype resembling that of wild-type. Alternatively, alteration of cellular shape and contacts may be linked to variation in rates of cell proliferation.

We then analysed SOX2 expression, cell proliferation and pituisphere formation in *p27*$^{-/-}$*;Sox2*$^{+/-}$ pituitaries (Fig2E-G). There is a visible reduction in SOX2 levels in *p27*$^{-/-}$*;Sox2*$^{+/-}$ IL (Fig2F and Supplementary Fig2B). Moreover EdU incorporation in compound mutants, both in melanotrophs and SCs is not significantly different from controls, in agreement with impaired tumour formation (Fig2E). A similar effect is observed in pituisphere assays (Fig2G).

Alteration of *p27*$^{-/-}$ melanotroph identity (Fig1G) also appears to depend on SOX2 dosage, because levels of *Tbx19* which are reduced in *p27*$^{-/-}$ IL , are not significantly affected in *p27*$^{-/-}$*;Sox2*$^{+/-}$

compared to control IL (Fig2H and 5K). However, levels of *Pomc* were still significantly reduced in *p27*$^{-/-}$;*Sox2*$^{+/-}$ IL compared to control.
Transcriptomic studies, proliferation and marker analyses all indicate that reduction of SOX2 dosage compromises at least most aspects of tumour genesis in *p27*$^{-/-}$ animals, implying an essential role for SOX2 in *p27*$^{-/-}$ melanotrophs and adjacent SCs for tumour development. To test whether the SOX2-P27 interaction relies solely on the *Srr2* enhancer [21], we generated mice deleted for this region (Fig2I-J). *Srr2*$^{del/del}$ mutants are viable (Supplementary Fig. 2C) and pituitary morphology is normal (Fig2K). However, on a *p27*$^{-/-}$ background, the *Srr2* deletion prevents tumorigenesis, while hyperplasia of IL is still evident as observed in *p27*$^{-/-}$;*Sox2*$^{+/-}$ mutants (Fig2K). In addition, the morphology of the retina, which is affected in absence of *p27* [17], is also improved in the *p27*$^{-/-}$; *Srr2*$^{del/del}$ mutants. In particular, and again similarly to *p27*$^{-/-}$;*Sox2*$^{+/-}$ mutants, the inner and outer layers have a reduced thickness and better organization compared to *p27*$^{-/-}$ retina (Fig2L) [21]. In the pituitary, levels of SOX2 are reduced in both melanotrophs and SCs in *p27*$^{-/-}$; *Srr2*$^{del/del}$ mutants compared to *p27*$^{-/-}$ samples (Fig2N). Intriguingly, EdU incorporation analyses reveal a specific reduction of proliferation in SCs in compound mutants compared to *p27*$^{-/-}$ samples (Fig2M). In agreement with this result, the efficiency of pituisphere formation from *p27*$^{-/-}$; *Srr2*$^{del/del}$ samples is more similar to control than *p27*$^{-/-}$samples (Fig2O). These analyses strongly suggest that *Srr2* has an exclusive role in mediating the SOX2-P27 interaction. Moreover, the consequences of its deletion are more obvious in SCs, suggesting that *Srr2* plays a more important role in this compartment. Furthermore, this implies that SCs may be critical for IL tumorigenesis in *p27*$^{-/-}$ mutants.

Requirement for SOX2 in *p27*$^{-/-}$ melanotrophs.

Conditional deletion of *p27* in melanotrophs results in formation of tumours, therefore transformation is cell-autonomous in this context [40]. To better characterise the role of SOX2 for tumour genesis, we deleted one copy of the gene exclusively in melanotrophs in *p27*$^{-/-}$ mutants. We initially used *Pomc-CreERT2* which displays a mosaic pattern of recombination in IL (Fig3A). To look at heterozygosity for *Sox2*, we induced Cre activity in four-week old *Pomc-CreERT2;Sox2*$^{fl/+}$;*p27*$^{-/-}$ animals and controls, which were then examined six to eight months later. Tumour development was unaffected by the mosaic deletion of one copy of *Sox2* in *p27*$^{-/-}$ melanotrophs (Fig3B). In agreement with this observation, proliferation was unaffected by *Sox2* reduction, as we observed a similar increase in EdU incorporation in *Pomc-CreERT2;Sox2*$^{fl/+}$;*p27*$^{-/-}$ and *Pomc-CreERT2;p27*$^{-/-}$ IL compared to controls (Fig3B,C). To analyse more directly the effect of the loss of one copy of *Sox2* on melanotrophs proliferative ability, we analysed EdU incorporation in *Pomc-CreERT2;Sox2*$^{fl/+}$;*p27*$^{-/-}$;*Rosa26*^{ReYFP} samples. We compared the percentages of eYFP;PAX7; EdU triple positive and eYFP negative, PAX7; EdU double positive melanotrophs, assuming that *Rosa26*^{ReYFP} recombination also reflected *Sox2* heterozygous deletion. We observed a significant reduction of EdU incorporation in eYFP positive versus negative cells (Fig3D). Therefore, reduction of SOX2 dosage in *p27*$^{-/-}$ melanotrophs diminishes their proliferative capacity.
We then hypothesized that a more efficient Cre-driver may block tumour formation; we therefore generated *Pomc-Cre;Sox2*$^{fl/+}$;*p27*$^{-/-}$animals. We showed previously that SOX2 is required for acquisition of melanotroph identity, however homozygous deletion of the gene once melanotrophs have up-regulated PAX7 does not have an apparent effect on cell fate acquisition [26]. There were no IL tumours or signs of hyperplasia in any four- to seven-month old *Pomc-Cre;Sox2*$^{fl/+}$;*p27*$^{-/-}$ animals (Fig 3F-H). Moreover POMC staining intensity was increased in *Pomc-Cre;Sox2*$^{fl/+}$;*p27*$^{-/-}$ melanotrophs compared to *p27*$^{-/-}$ samples (Fig3I), indicating restoration of a normal melanotroph

phenotype. This demonstrates that SOX2 is required in melanotrophs for *p27* deletion to result in tumourigenesis. Strikingly, the morphology of IL appears completely normal in *Pomc-Cre;Sox2*$_{fl/+}$*;p27*$_{-/-}$ (Fig3F,G) compared to *p27*$_{-/-}$*;Sox2*$_{+/-}$ IL where hyperplasia is clear (Fig2A). This difference in phenotype is unexpected, because in both mutants the genotype of melanotrophs is the same: only one allele of *Sox2* is active while *p27* is deleted. However, different regulatory mechanisms may affect the levels of expression of the remaining copy of *Sox2* in *Pomc-Cre;Sox2*$_{fl/+}$*;p27*$_{-/-}$ versus *p27*$_{-/-}$*;Sox2*$_{+/-}$ melanotrophs. We thus quantified *Sox2* levels and observe an up-regulation in *p27*$_{-/-}$, and to a lesser extent in *p27*$_{-/-}$*;Sox2*$_{+/-}$ samples (Fig3J,K). In agreement with the absence of hyperplasia, we observed a further reduction in *Sox2* expression in *Pomc-Cre;Sox2*$_{fl/+}$*;p27*$_{-/-}$ versus *p27*$_{-/-}$*;Sox2*$_{+/-}$ samples, suggesting that regulation of *Sox2* is indeed modulated according to the spatio-temporal pattern of its deletion. Furthermore we also observe, albeit to a lesser extent, reduction of *Sox2* expression in *Pomc-Cre;Sox2*$_{fl/+}$*;p27*$_{-/-}$ SCs.
In conclusion, SOX2 is required cell-autonomously in melanotrophs for tumour development in *p27*$_{-/-}$ mutants. Moreover, reduction of *Sox2* expression in SCs in *Pomc-Cre;Sox2*$_{fl/+}$*;p27*$_{-/-}$ suggests a non cell autonomous role, and implies an interaction between melanotrophs and SCs.

SOX2 is required in SCs for melanotroph tumour induction in *p27*$_{-/-}$ animals.

Because deletion of *p27* induces up-regulation of SOX2 in SCs, we specifically wished to ask whether the SCs flanking the IL directly give rise to tumour cells or induce tumour formation. Given that, in the context of the pituitary, SOX9 is expressed uniquely in the SCs (Fauquier et al., 2008), we first performed lineage tracing experiments using *Sox9*$_{iresCreERT2}$ [41]. Cre activity was induced in four-week-old *Sox9*$_{iresCreERT2/+}$*;Rosa26*$_{ReYFP/+}$ animals and pituitaries harvested six to eight months later. In controls, the vast majority of eYFP positive cells are SOX9 positive SCs [28] (Fig4A). In agreement with a low turnover of melanotrophs [12], very few eYFP positive cells are present in IL (Fig4A); these are negative for SOX9 and PAX7, where the latter indicates they are not melanotrophs. Their identity is unclear; they may originate from the pituitary SC layer or the posterior lobe where SOX9 is also expressed. In *p27*$_{-/-}$ animals we also observe that most eYFP positive cells are SOX9 positive SCs. However, in contrast with *Sox9*$_{iresCreERT2/+}$*;Rosa26*$_{ReYFP/+}$ controls, we observe some rare eYFP;PAX7 positive melanotrophs. This shows that while SCs are not at the origin of the melanotroph tumours in *p27*$_{-/-}$ animals, tumour formation and/or lack of *p27* in SCs, drives commitment of a few SCs toward the melanotroph lineage.
To investigate the role of SOX2 in SCs during tumourigenesis one allele of the gene was removed in *Sox9*$_{iresCreERT2/+}$*;Sox2*$_{fl/+}$*;p27*$_{-/-}$ animals. Cre activity was induced in four-week old animals and pituitaries harvested when the animals were six- to twelve-month old. While the IL is consistently hyperplastic in *Sox9*$_{iresCreERT2/+}$*;Sox2*$_{fl/+}$*;p27*$_{-/-}$ animals, similarly to *p27*$_{-/-}$*;Sox2*$_{+/-}$ mice, only one amongst seven 12-month old animals of the former genotype developed an IL tumour, while all *p27*$_{-/-}$controls were affected (Fig4B, upper panel). The thickness of the SOX2 positive SC layer appeared reduced in *Sox9*$_{iresCreERT2/+}$*;Sox2*$_{fl/+}$*;p27*$_{-/-}$ compared to *Sox9*$_{iresCreERT2/+}$*;p27*$_{-/-}$ (Fig4B, lower panel), and there were fewer SCs upon *Sox2* reduction (Supplementary Fig3A). SOX2 staining intensity in SC was also reduced (Fig4F, Supplementary Fig3B). Furthermore, we observed a significant reduction of proliferation in both SC and melanotrophs in six-month old *Sox9*$_{iresCreERT2/+}$*;Sox2*$_{fl/+}$*;p27*$_{-/-}$ IL compared to *Sox9*$_{iresCreERT2/+}$*; p27*$_{-/-}$ samples (Fig4C, D, F). In addition, formation of ectopic vascular structures is significantly decreased (Fig4E, F).

These findings indicate that SOX2 activity in the SCs, and consequently the SCs themselves, are required for tumourigenesis in *p27*$^{-/-}$ IL. *Sox2* dosage therefore impacts on *p27*$^{-/-}$ melanotrophs, both cell-autonomously and indirectly.

Characterization of the transcriptional consequences of altering *Sox2* levels in *p27*$^{-/-}$ IL SCs.

We performed single cell RNA sequencing analysis (scRNAseq) on ILs from three-month old *Sox9*$^{iresCreERT2/+}$, *Sox9*$^{iresCreERT2/+}$*;p27*$^{-/-}$ and *Sox9*$^{iresCreERT2/+}$*;Sox2*$^{fl/+}$*;p27*$^{-/-}$ animals, where Cre activity had been induced at birth. Dataset clustering was performed by generating UMAP plots (Fig5A). The three datasets were integrated and clusters identified according to the expression of known DEG, and by comparison with published studies [31,42]. The major cell cluster corresponds to melanotrophs as expected (*Tbx19*, *Pomc* and *Pax7* positive). The SC cluster (*Sox2*, *Sox9* positive) is proportionally larger in our IL dataset in comparison with studies performed on the whole pituitary [31,42]. We independently re-analysed the SC (Fig5C, D) and melanotroph clusters (Fig5G, H). Within each cell type we observed that cells were mostly, but not perfectly, clustered according to their genotype. We thus aimed at examining DEGs between the clusters to characterise the direct effect of *Sox2* dosage on SCs, and the consequences on melanotrophs. More precisely, we analysed DEGs in *Sox9*$^{iresCreERT2/+}$*;p27*$^{-/-}$ compared to *Sox9*$^{iresCreERT2/+}$ and *Sox9*$^{iresCreERT2/+}$*;Sox2*$^{fl/+}$*;p27*$^{-/-}$.
In SCs, (Fig5C, D) thirty-six DEGs were identified by comparing subcluster 1 (which has the highest proportion of *p27*$^{-/-}$ cells) to the two other subclusters (Supplementary Table 1). Thirty of the DEGs were upregulated in subcluster 1, and amongst them, fourteen have been associated with tumorigenesis (Fig5E). Amongst these, five are immediate early response genes (*Ier2*, *Fos*, *Junb*, *Jun* and *Egr1*) that can be activated by the MAPK pathway. Activation of the pathway in embryonic pituitary progenitors is associated with expansion of this compartment [43]. We thus performed immunohistochemistry for phosphorylated ERK and observe a clear and specific upregulation of the signal in *p27*$^{-/-}$ SCs, in contrast with both control and *Sox9*$^{iresCreERT2/+}$*;Sox2*$^{fl/+}$*;p27*$^{-/-}$ samples (Fig5F). This suggests that SOX2 positively regulates activity of the pathway in SCs, either directly or indirectly, and this correlates with tumourigenesis.
Subclustering of the melanotrophs, which were more numerous than the SCs, was better associated with the different genotypes (Fig5G, H). In agreement with the absence of tumour formation, there was a reduction in melanotroph numbers in *Sox9*$^{iresCreERT2/+}$*;Sox2*$^{fl/+}$*;p27*$^{-/-}$ compared to *Sox9*$^{iresCreERT2/+}$*;p27*$^{-/-}$, but these were still more numerous than in wild-type, in agreement with the hyperplasia observed in compound mutants (Fig5G). Furthermore, while melanotrophs are genetically equivalent in *Sox9*$^{iresCreERT2/+}$*;p27*$^{-/-}$ and *Sox9*$^{iresCreERT2/+}$*;Sox2*$^{fl/+}$*;p27*$^{-/-}$ samples, their transcriptome is clearly different, further confirming the SOX2-dependent effect of SCs on melanotrophs. There were 624 DEGS in cluster 0 (*Sox9*$^{iresCreERT2/+}$*;p27*$^{-/-}$) melanotrophs compared to clusters 2 (*Sox9*$^{iresCreERT2/+}$) and 1 (*Sox9*$^{iresCreERT2/+}$*;Sox2*$^{fl/+}$*;p27*$^{-/-}$) (Fig5I). Pathway analysis of the 593 downregulated genes in *Sox9*$^{iresCreERT2/+}$*;p27*$^{-/-}$ melanotrophs revealed that vesicular and endosomal traffic, and cytoskeleton remodelling were predominantly affected, suggesting that the differentiated, secretory phenotype of melanotrophs was restored upon reduction of SOX2 in SCs (Fig5J, upper). In agreement with this hypothesis, *Tbx19* was amongst the downregulated genes in *Sox9*$^{iresCreERT2/+}$*;p27*$^{-/-}$ melanotrophs. Recovery of normal expression levels of *Tbx19* upon *Sox2* downregulation in SCs was further validated by quantitative PCR (Fig5K). Finally, pairwise comparison between cluster 0 and 1, comprising *Sox9*$^{iresCreERT2/+}$*;p27*$^{-/-}$ and *Sox9*$^{iresCreERT2/+}$*;Sox2*$^{fl/+}$*;p27*$^{-/-}$ cells respectively, revealed a significant enrichment in process networks associated with translation and transcription (Fig5J, bottom), suggesting reduced levels of

both transcription and translation in *p27*$^{-/-}$ cells, restored in melanotrophs upon reduction of *Sox2* levels in SCs. SCs and CSCs are known to have reduced levels of translation. Moreover, SOX2 was recently shown to be directly involved in alterations in the rate of protein synthesis in a mouse model of squamous tumour initiating cells [44]. This suggests that SOX2 may play a similar role in *p27*$^{-/-}$ melanotrophs, acting as a repressor of translation and transcription of genes related to differentiation. Altogether these data show that SOX2 upregulation in *p27*$^{-/-}$ SCs results in the induction of a dedifferentiated, pro-tumoral phenotype in melanotrophs. In SCs, SOX2 overexpression leads to increased MAPK pathway activation, which correlates with and may mediate the role of SOX2 in tumorigenesis, at least in *p27*$^{-/-}$ IL, but maybe also in other contexts.

Discussion

The regulation of *Sox2* expression is extremely complex [45] and variation of its expression levels have contrasting consequences in cancers [23]. We previously uncovered that P27 drives *Sox2* repression and that deletion of one copy of *Sox2* in *p27*$^{-/-}$ animals rescues deleterious aspects of the *p27*$^{-/-}$ phenotype, in particular tumours of the pituitary, which are the most frequent cancers in this model [21]. Here we have further dissected the role of SOX2, and also demonstrated the importance of *Srr2* for the SOX2-P27 interaction. We have shown that SOX2 is required independently in both melanotrophs and SCs for IL tumours to develop in *p27*$^{-/-}$ animals. The requirement for SOX2 in SCs is particularly interesting, because it implies that SCs, upon loss of P27, act on melanotrophs to promote tumour formation. To better analyse this aspect, we performed a single cell transcriptomic analysis to simultaneously explore the SOX2-dependent tumour inducing effect within SCs, and the consequences for melanotrophs. These analyses revealed that in *p27*$^{-/-}$ SCs, SOX2 upregulation leads to MAPK pathway overactivation. In melanotrophs, increased proliferation and alteration of endocrine cell identity is mediated by the SCs, and this correlates with tumour formation. The pleiotropic, pro-tumorigenic effects of SOX2 in distinct cell types in the absence of P27 demonstrate that it is a crucial mediator of tumourigenesis and hence, as suggested before, a good target for anti-tumoral treatments. However, we also show that SOX2 only appears to be a relevant target in a subset of tissues when P27 is lost or its expression decreased, such as the pituitary and duodenum. It would be interesting to examine whether SCs are able to induce tumour development in the others organs comprised in this subset, as they do in the pituitary.

Understanding the reasons behind the tissue specificity for the SOX2-P27 interaction could help to define pre-existing factors favoring tumorigenesis. Our results suggest that derepression of *Sox2* in the absence of P27 leads to IL tumours. However this happens only in some cell types, while expression of *p27* is ubiquitous, likely illustrating the multiple anti-proliferative roles of P27 that are distinct from *Sox2* repression [46,47]. Differential expression of P27 interactors and/or targets, and of other cell cycle repressors may explain tissue-specific features of the *p27*$^{-/-}$ phenotype.

In pituitary endocrine cells, maintenance of SOX2 expression appears to be a prerequisite for tumoral development in absence of *p27*, since melanotrophs are the only such cell type to maintain its expression [26]. While melanotrophs are also uniquely characterized by their non-proliferative status [12], levels of P27 are unexpectedly relatively low in melanotrophs. This suggests that in *p27*$^{-/-}$ mutants, an active *Sox2* locus normally under P27 control, coupled with a relaxed control of the cell-cycle renders melanotrophs particularly prone to tumorigenesis. In agreement, independent deletion of genes encoding for different negative cell cycle regulators show that IL is particularly sensitive to tumoral development [13]. Furthermore derepression of *Sox2* is also observed in *pRb*$^{+/-}$ pituitary tumors [48]. It would be interesting to examine whether SOX2 is required for IL tumorigenesis in other cell cycle regulator mutants. Conversely we can now screen for cell types satisfying the relevant criteria, including low cell-turnover, low negative cell cycle regulator levels, and presence of SOX2, and examine for tumorigenic potential.

Our study highlights common and cell-specific roles of SOX2 during tumorigenesis. Both in *p27*$^{-/-}$ melanotrophs and SCs, SOX2 upregulation is associated with overproliferation. The association of SOX2 with dedifferentiation and overproliferation has been observed in many tumours [23], as we also observe here in melanotrophs. In pituitary SCs, our results suggest that this overproliferation is linked to MAPK overactivation, something that has been shown in embryonic pituitaries expressing an activated form of *Braf* [43]. How SOX2 derepression induces MAPK activation is less clear; MAPK pathway activation has been linked to induction of *Sox2* expression [49], but the molecular mechanisms undelying the converse have not been characterized. While SOX2 has been associated with CSC

properties in some other tumours [50], we report here its requirement in SCs for these to promote tumorigenesis in neighbouring melanotrophs. Although the low number of SCs comprised in our single cell analysis may have precluded the characterization of many more differentially expressed genes, increased expression of *Hes1* was observed, suggesting increased activity of the Notch pathway. While the opposite result, i.e. reduced expression of some Notch pathway genes in *p27*$^{-/-}$ mutants, was seen in the bulk RNAseq results; this most likely reflects the much lower proportion of SCs in the bulk sample as melanotroph numbers become disproportionally higher. In pituitary SCs, the Notch pathway is active [51] and required for maintenance of SOX2 positive SCs [52,53]. In other contexts, SOX2 has been shown to directly regulate the expression of Notch pathway genes [54,55], which is consistent with our single cell data. Notch pathway activation can result in induction of a tumoral phenotype in surrounding cells, in particular by increasing cytokine expression [56,57]. Manipulation of MAPK and Notch pathways in SC in *p27*$^{-/-}$ animals is now required to characterise their effect on SCs and melanotroph transformation.

In parallel with the partial melanotroph dedifferentiation observed here, we previously reported a very clear dedifferentiation of melanotrophs and corticotrophs following cell autonomous NOTCH pathway activation [58]. While NOTCH is unlikely to be involved cell-autonomoulsy here, it is remarkable that we also observed increased expression of SOX2 in dedifferentiating melanotrophs. The POMC lineage was the only pituitary lineage to display such plasticity, suggesting that in addition to being more sensitive to situations where proliferative control is unlocked, melanotroph fate is also relatively unstable. The importance of this SOX2-dependent plasticity was recently demonstrated in prostate cancer where cell-autonomous derepression of SOX2 induces a cell fate change underlying chemoresistance [24,25].

To further characterise the molecular mechanisms involved in the SOX2-P27 interaction, we have deleted *Srr2*. SOX2 itself, c-myc and members of the POU transcription factor family bind to *Srr2* to promote expression of the gene [59]. Beside P27 [21], other negative regulators of *Srr2* have been characterised such as P21 in neural SCs [60] and pRb in the pituitary [48]. Analysis of *p27*$^{-/-}$*; Srr2*$^{del/del}$ animals show that the repressive action of P27 is mediated by *Srr2* and in absence of *p27*, Srr2 activators drive *Sox2* expression; this then leads to pituitary tumours and retina defects (see model, supplementary Fig4). Notably, loss of *Srr2* affects cell proliferation exclusively in *p27*$^{-/-}$ SCs, suggesting that the role of the enhancer is more important in SCs, in agreement with a role for these in promoting the melanotroph tumours. Further analysis of these animals is required to assess the tissue-specific roles of *Srr2*, particularly in neural SCs where this enhancer is active [61,60] (Domingo-Muelas A., M-A V. et al, *in preparation*).

In conclusion, our study reveals how *Sox2* derepression, independently in two adjacent cell types, underlies tumorigenesis in one of them. Moreover, our work reveals the existence of reciprocal interactions between melanotrophs and flanking SCs to orchestrate tumour development. This highlights the complexity of the mechanisms triggering tumorigenesis and the central role of SOX2 in this process. Furthermore pituitary SCs, which are not tumoral, but have a tumour inducing activity, represent good anti-tumoural treatment targets, highlighting the importance of detailed characterisation of mechanisms underlying tumour formation to decipher possible anti-tumour strategies.

Acknowledgements

We are grateful for help and support from all members of the Lovell-Badge's lab. We thank Jacques Drouin (Institut de Recherches Cliniques de Montreal) for sharing the Pomc-Cre animals and the pituitary *Pomc* regulatory element; Francis Poulat (Institut de Génétique Humaine, Montpellier) for the generous gift of SOX9 antibody; and Donald Bell for his expertise on image quantification. We are grateful to Dr. A.F. Parlow and the NHPP for reagents for the sandwich ELISA and immunofluorescence experiments. We also thank Biological Services, Flow cytometry, Advanced Sequencing, and Advanced light microscopy platforms at the Francis Crick Institute, for their excellent assistance and technical support.
This work was supported by the Medical Research Council, U.K. (U117512772, U117562207 and U117570590), the Francis Crick Institute which receives its core funding from Cancer Research UK (FC001107), the UK Medical Research Council (FC001107), and the Wellcome Trust (FC001107), and the Worldwide Cancer Research charity (grant 13-1270).

Bibliography

1 Baghban, R. *et al.* Tumor microenvironment complexity and therapeutic implications at a glance. *Cell Commun Signal* **18**, 59, doi:10.1186/s12964-020-0530-4 (2020).

2 Lytle, N. K., Barber, A. G. & Reya, T. Stem cell fate in cancer growth, progression and therapy resistance. *Nat Rev Cancer* **18**, 669-680, doi:10.1038/s41568-018-0056-x (2018).

3 Balbinot, C. *et al.* The Cdx2 homeobox gene suppresses intestinal tumorigenesis through non-cell-autonomous mechanisms. *J Exp Med* **215**, 911-926, doi:10.1084/jem.20170934 (2018).

4 Lujambio, A. *et al.* Non-cell-autonomous tumor suppression by p53. *Cell* **153**, 449-460, doi:10.1016/j.cell.2013.03.020 (2013).

5 Mescher, M. *et al.* The epidermal polarity protein Par3 is a non-cell autonomous suppressor of malignant melanoma. *J Exp Med* **214**, 339-358, doi:10.1084/jem.20160596 (2017).

6 Kode, A. *et al.* Leukaemogenesis induced by an activating beta-catenin mutation in osteoblasts. *Nature* **506**, 240-244, doi:10.1038/nature12883 (2014).

7 Andoniadou, C. L. *et al.* Sox2(+) stem/progenitor cells in the adult mouse pituitary support organ homeostasis and have tumor-inducing potential. *Cell Stem Cell* **13**, 433-445, doi:10.1016/j.stem.2013.07.004 (2013).

8 Tanaka, S. *et al.* Angiogenesis in the intermediate lobe of the pituitary gland alters its structure and function. *Gen Comp Endocrinol* **185**, 10-18, doi:10.1016/j.ygcen.2013.01.009 (2013).

9 Drouin, J. 60 YEARS OF POMC: Transcriptional and epigenetic regulation of POMC gene expression. *J Mol Endocrinol* **56**, T99-T112, doi:10.1530/JME-15-0289 (2016).

10 Lamolet, B. *et al.* A pituitary cell-restricted T box factor, Tpit, activates POMC transcription in cooperation with Pitx homeoproteins. *Cell* **104**, 849-859 (2001).

11 Budry, L. *et al.* The selector gene Pax7 dictates alternate pituitary cell fates through its pioneer action on chromatin remodeling. *Genes Dev* **26**, 2299-2310, doi:10.1101/gad.200436.112 (2012).

12 Langlais, D., Couture, C., Kmita, M. & Drouin, J. Adult pituitary cell maintenance: lineage-specific contribution of self-duplication. *Mol Endocrinol* **27**, 1103-1112, doi:10.1210/me.2012-1407 (2013).

13 Quereda, V. & Malumbres, M. Cell cycle control of pituitary development and disease. *J Mol Endocrinol* **42**, 75-86, doi:JME-08-0146 [pii] 10.1677/JME-08-0146 (2009).

14 Sharma, S. S. & Pledger, W. J. The non-canonical functions of p27(Kip1) in normal and tumor biology. *Cell Cycle* **15**, 1189-1201, doi:10.1080/15384101.2016.1157238 (2016).

15 Fero, M. L. *et al.* A syndrome of multiorgan hyperplasia with features of gigantism, tumorigenesis, and female sterility in p27(Kip1)-deficient mice. *Cell* **85**, 733-744, doi:S0092-8674(00)81239-8 [pii] (1996).

16 Kiyokawa, H. *et al.* Enhanced growth of mice lacking the cyclin-dependent kinase inhibitor function of p27(Kip1). *Cell* **85**, 721-732, doi:S0092-8674(00)81238-6 [pii] (1996).

17 Nakayama, K. *et al.* Mice lacking p27(Kip1) display increased body size, multiple organ hyperplasia, retinal dysplasia, and pituitary tumors. *Cell* **85**, 707-720, doi:S0092-8674(00)81237-4 [pii] (1996).

18 Alrezk, R., Hannah-Shmouni, F. & Stratakis, C. A. MEN4 and CDKN1B mutations: the latest of the MEN syndromes. *Endocrine-related cancer* **24**, T195-T208, doi:10.1530/ERC-17-0243 (2017).

19 Bilodeau, S., Roussel-Gervais, A. & Drouin, J. Distinct developmental roles of cell cycle inhibitors p57Kip2 and p27Kip1 distinguish pituitary progenitor cell cycle exit from cell cycle reentry of differentiated cells. *Mol Cell Biol* **29**, 1895-1908, doi:MCB.01885-08 [pii] 10.1128/MCB.01885-08 (2009).

20 Tong, W. & Pollard, J. W. Genetic evidence for the interactions of cyclin D1 and p27(Kip1) in mice. *Mol Cell Biol* **21**, 1319-1328, doi:10.1128/MCB.21.4.1319-1328.2001 (2001).

21 Li, H. *et al.* p27(Kip1) directly represses Sox2 during embryonic stem cell differentiation. *Cell Stem Cell* **11**, 845-852, doi:10.1016/j.stem.2012.09.014 (2012).
22 Sarkar, A. & Hochedlinger, K. The sox family of transcription factors: versatile regulators of stem and progenitor cell fate. *Cell Stem Cell* **12**, 15-30, doi:10.1016/j.stem.2012.12.007 (2013).
23 Wuebben, E. L. & Rizzino, A. The dark side of SOX2: cancer - a comprehensive overview. *Oncotarget* **8**, 44917-44943, doi:10.18632/oncotarget.16570 (2017).
24 Ku, S. Y. *et al.* Rb1 and Trp53 cooperate to suppress prostate cancer lineage plasticity, metastasis, and antiandrogen resistance. *Science* **355**, 78-83, doi:10.1126/science.aah4199 (2017).
25 Mu, P. *et al.* SOX2 promotes lineage plasticity and antiandrogen resistance in TP53- and RB1-deficient prostate cancer. *Science* **355**, 84-88, doi:10.1126/science.aah4307 (2017).
26 Goldsmith, S., Lovell-Badge, R. & Rizzoti, K. SOX2 is sequentially required for progenitor proliferation and lineage specification in the developing pituitary. *Development* **143**, 2376-2388, doi:10.1242/dev.137984 (2016).
27 Fauquier, T., Rizzoti, K., Dattani, M., Lovell-Badge, R. & Robinson, I. C. SOX2-expressing progenitor cells generate all of the major cell types in the adult mouse pituitary gland. *Proc Natl Acad Sci U S A* **105**, 2907-2912, doi:0707886105 [pii] 10.1073/pnas.0707886105 (2008).
28 Rizzoti, K., Akiyama, H. & Lovell-Badge, R. Mobilized adult pituitary stem cells contribute to endocrine regeneration in response to physiological demand. *Cell Stem Cell* **13**, 419-432, doi:10.1016/j.stem.2013.07.006 (2013).
29 Sherr, C. J. & Roberts, J. M. CDK inhibitors: positive and negative regulators of G1-phase progression. *Genes Dev* **13**, 1501-1512, doi:10.1101/gad.13.12.1501 (1999).
30 Levy, A. Physiological implications of pituitary trophic activity. *J Endocrinol* **174**, 147-155, doi:JOE04773 [pii] (2002).
31 Mayran, A. *et al.* Pioneer and nonpioneer factor cooperation drives lineage specific chromatin opening. *Nature communications* **10**, 3807, doi:10.1038/s41467-019-11791-9 (2019).
32 Nantie, L. B., Himes, A. D., Getz, D. R. & Raetzman, L. T. Notch signaling in postnatal pituitary expansion: proliferation, progenitors, and cell specification. *Mol Endocrinol* **28**, 731-744, doi:10.1210/me.2013-1425 (2014).
33 Aster, J. C., Pear, W. S. & Blacklow, S. C. The Varied Roles of Notch in Cancer. *Annu Rev Pathol* **12**, 245-275, doi:10.1146/annurev-pathol-052016-100127 (2017).
34 Lodge, E. J. *et al.* Homeostatic and tumourigenic activity of SOX2+ pituitary stem cells is controlled by the LATS/YAP/TAZ cascade. *Elife* **8**, doi:10.7554/eLife.43996 (2019).
35 Besson, A., Gurian-West, M., Schmidt, A., Hall, A. & Roberts, J. M. p27Kip1 modulates cell migration through the regulation of RhoA activation. *Genes Dev* **18**, 862-876, doi:10.1101/gad.1185504 (2004).
36 Borrelli, E., Heyman, R. A., Arias, C., Sawchenko, P. E. & Evans, R. M. Transgenic mice with inducible dwarfism. *Nature* **339**, 538-541, doi:10.1038/339538a0 (1989).
37 Pulichino, A. M. *et al.* Tpit determines alternate fates during pituitary cell differentiation. *Genes Dev* **17**, 738-747, doi:10.1101/gad.1065703 (2003).
38 Kelberman, D. *et al.* Mutations within Sox2/SOX2 are associated with abnormalities in the hypothalamo-pituitary-gonadal axis in mice and humans. *J Clin Invest* **116**, 2442-2455, doi:10.1172/JCI28658 (2006).
39 Jayakody, S. A. *et al.* SOX2 regulates the hypothalamic-pituitary axis at multiple levels. *The Journal of clinical investigation* **122**, 3635-3646, doi:10.1172/JCI64311 (2012).
40 Chien, W. M. *et al.* Genetic mosaics reveal both cell-autonomous and cell-nonautonomous function of murine p27Kip1. *Proc Natl Acad Sci U S A* **103**, 4122-4127, doi:10.1073/pnas.0509514103 (2006).
41 Furuyama, K. *et al.* Continuous cell supply from a Sox9-expressing progenitor zone in adult liver, exocrine pancreas and intestine. *Nat Genet* **43**, 34-41, doi:ng.722 [pii] 10.1038/ng.722 (2010).

42 Cheung, L. Y. M. *et al.* Single-Cell RNA Sequencing Reveals Novel Markers of Male Pituitary Stem Cells and Hormone-Producing Cell Types. *Endocrinology* **159**, 3910-3924, doi:10.1210/en.2018-00750 (2018).
43 Haston, S. *et al.* MAPK pathway control of stem cell proliferation and differentiation in the embryonic pituitary provides insights into the pathogenesis of papillary craniopharyngioma. *Development* **144**, 2141-2152, doi:10.1242/dev.150490 (2017).
44 Sendoel, A. *et al.* Translation from unconventional 5' start sites drives tumour initiation. *Nature* **541**, 494-499, doi:10.1038/nature21036 (2017).
45 Kondoh, I. & Lovell-Badge, R. *Sox2 Biology and role in development and disease*. (Elsevier, 2015).
46 Fabris, L. *et al.* p27kip1 controls H-Ras/MAPK activation and cell cycle entry via modulation of MT stability. *Proc Natl Acad Sci U S A* **112**, 13916-13921, doi:10.1073/pnas.1508514112 (2015).
47 Nguyen, L. *et al.* p27kip1 independently promotes neuronal differentiation and migration in the cerebral cortex. *Genes Dev* **20**, 1511-1524, doi:10.1101/gad.377106 (2006).
48 Vilas, J. M. *et al.* Transcriptional regulation of Sox2 by the retinoblastoma family of pocket proteins. *Oncotarget* **6**, 2992-3002, doi:10.18632/oncotarget.2996 (2015).
49 Wang, K. *et al.* FGFR1-ERK1/2-SOX2 axis promotes cell proliferation, epithelial-mesenchymal transition, and metastasis in FGFR1-amplified lung cancer. *Oncogene* **37**, 5340-5354, doi:10.1038/s41388-018-0311-3 (2018).
50 Schaefer, T. & Lengerke, C. SOX2 protein biochemistry in stemness, reprogramming, and cancer: the PI3K/AKT/SOX2 axis and beyond. *Oncogene* **39**, 278-292, doi:10.1038/s41388-019-0997-x (2020).
51 Chen, J., Crabbe, A., Van Duppen, V. & Vankelecom, H. The notch signaling system is present in the postnatal pituitary: marked expression and regulatory activity in the newly discovered side population. *Mol Endocrinol* **20**, 3293-3307, doi:me.2006-0293 [pii] 10.1210/me.2006-0293 (2006).
52 Zhu, X., Tollkuhn, J., Taylor, H. & Rosenfeld, M. G. Notch-Dependent Pituitary SOX2(+) Stem Cells Exhibit a Timed Functional Extinction in Regulation of the Postnatal Gland. *Stem Cell Reports* **5**, 1196-1209, doi:10.1016/j.stemcr.2015.11.001 (2015).
53 Batchuluun, K., Azuma, M., Fujiwara, K., Yashiro, T. & Kikuchi, M. Notch Signaling and Maintenance of SOX2 Expression in Rat Anterior Pituitary Cells. *Acta Histochem Cytochem* **50**, 63-69, doi:10.1267/ahc.17002 (2017).
54 Taranova, O. V. *et al.* SOX2 is a dose-dependent regulator of retinal neural progenitor competence. *Genes Dev* **20**, 1187-1202, doi:20/9/1187 [pii] 10.1101/gad.1407906 (2006).
55 Zhou, C. *et al.* Comprehensive profiling reveals mechanisms of SOX2-mediated cell fate specification in human ESCs and NPCs. *Cell Res* **26**, 171-189, doi:10.1038/cr.2016.15 (2016).
56 Colombo, M. *et al.* Cancer Cells Exploit Notch Signaling to Redefine a Supportive Cytokine Milieu. *Front Immunol* **9**, 1823, doi:10.3389/fimmu.2018.01823 (2018).
57 Meurette, O. & Mehlen, P. Notch Signaling in the Tumor Microenvironment. *Cancer Cell* **34**, 536-548, doi:10.1016/j.ccell.2018.07.009 (2018).
58 Cheung, L. *et al.* NOTCH activity differentially affects alternative cell fate acquisition and maintenance. *Elife* **7**, doi:10.7554/eLife.33318 (2018).
59 Miyagi, S. *et al.* The Sox-2 regulatory regions display their activities in two distinct types of multipotent stem cells. *Mol Cell Biol* **24**, 4207-4220 (2004).
60 Marques-Torrejon, M. A. *et al.* Cyclin-dependent kinase inhibitor p21 controls adult neural stem cell expansion by regulating Sox2 gene expression. *Cell Stem Cell* **12**, 88-100, doi:10.1016/j.stem.2012.12.001 (2013).
61 Miyagi, S. *et al.* The Sox2 regulatory region 2 functions as a neural stem cell-specific enhancer in the telencephalon. *J Biol Chem* **281**, 13374-13381, doi:10.1074/jbc.M512669200 (2006).

62 Srinivas, S. *et al.* Cre reporter strains produced by targeted insertion of EYFP and ECFP into the ROSA26 locus. *BMC Dev Biol* **1**, 4 (2001).
63 Gonen, N. *et al.* Sex reversal following deletion of a single distal enhancer of Sox9. *Science* **360**, 1469-1473, doi:10.1126/science.aas9408 (2018).
64 Rizzoti, K. *et al.* SOX3 is required during the formation of the hypothalamo-pituitary axis. *Nat Genet* **36**, 247-255 (2004).
65 Barratt, C. L. R. *et al.* The diagnosis of male infertility: an analysis of the evidence to support the development of global WHO guidance-challenges and future research opportunities. *Hum Reprod Update* **23**, 660-680, doi:10.1093/humupd/dmx021 (2017).
66 Furlan, A. *et al.* Multipotent peripheral glial cells generate neuroendocrine cells of the adrenal medulla. *Science* **357**, doi:10.1126/science.aal3753 (2017).
67 Bankhead, P. *et al.* QuPath: Open source software for digital pathology image analysis. *Sci Rep* **7**, 16878, doi:10.1038/s41598-017-17204-5 (2017).
68 Livak, K. J. & Schmittgen, T. D. Analysis of relative gene expression data using real-time quantitative PCR and the 2(-Delta Delta C(T)) Method. *Methods* **25**, 402-408, doi:10.1006/meth.2001.1262 (2001).
69 McGuinness, L. *et al.* Autosomal dominant growth hormone deficiency disrupts secretory vesicles in vitro and in vivo in transgenic mice. *Endocrinology* **144**, 720-731 (2003).
70 Li, B. & Dewey, C. N. RSEM: accurate transcript quantification from RNA-Seq data with or without a reference genome. *BMC Bioinformatics* **12**, 323, doi:10.1186/1471-2105-12-323 (2011).
71 Dobin, A. *et al.* STAR: ultrafast universal RNA-seq aligner. *Bioinformatics* **29**, 15-21, doi:10.1093/bioinformatics/bts635 (2013).
72 Love, M. I., Huber, W. & Anders, S. Moderated estimation of fold change and dispersion for RNA-seq data with DESeq2. *Genome Biol* **15**, 550, doi:10.1186/s13059-014-0550-8 (2014).
73 Team, R. D. C. R: A language and environment for statistical computing. . *R Foundation for Statistical Computing, Vienna, Austria.* (2008).
74 Stuart, T. *et al.* Comprehensive Integration of Single-Cell Data. *Cell* **177**, 1888-1902 e1821, doi:10.1016/j.cell.2019.05.031 (2019).

Material and Methods

Ethics Statement

All experiments carried out on mice were approved under the UK Animal (scientific procedures) Act (Project licence 80/2405 and 70/8560).

Mice

Cdkn1b$_{tm1Mlf}$ (*p27-*) [15], *Sox9*$_{tm1(cre/ERT2)Haak}$ (*Sox9*$_{iresCreERT2}$) [41], *Tg(PomC-Cre)Dro* (*Pomc-Cre)* [12], *Sox2*$_{tm1Lpev}$ (Sox2$_{GFP}$), *Sox2*$_{tm2Lpev}$ (Sox2$_{fl}$) [54] and *Gt(ROSA)26Sor*$_{tm1(EYFP)Cos}$ (*Rosa26*$_{ReYFP}$) [62] were maintained on mixed background. Experiments were either performed using littermates or animals with comparable backgrounds.

Cre activity was induced by tamoxifen administration for 3 consecutive days at 5mg/25g body weight /day. Pituitaries were harvested after tamoxifen treatment, as indicated in each experiment. Genotyping was performed by Transnetyx®.

Generation of Pomc-CreERT2 transgenic mice and and *Sox2* $_{tm1(Guide1/1:SRR2)RLB}$ mice

Tg(Pomc-cre/ERT2)Rlb (*Pomc-CreERT2*) mice were generated by inserting a 543bp (-480/+63) region of the *Pomc* promoter [12] upstream of the sequence coding for iCreERT2. *Pomc-CreERT2* animals were obtained by standard pronuclear injection. Tissue-specific activity of Pomc-CreERT2 was confirmed by crossing transgene positive animals with *Rosa26*$_{ReYFP/ReYFP}$ mice; one founder was chosen to establish the strain.

The *Sox2* $_{tm1(Guide1/1:SRR2)RLB}$ allele was generated using the CRISPR/Cas9 technology. Single guide RNAs (sgRNAs) were designed (www.crispr.mit.edu) to induce deletion of the mouse SRR2 enhancer (81 bp), situated 4kb downstream of *Sox2* (UCSC mm9 genome chr13: 34,552,926 - 34,553,007). Two pairs of guides were designed: pair 1(G1_5'+G1_3') and pair 2 (G4_5'+G5_3') (Table S2) and independently injected into zygotes with Cas9 mRNA as previously described [63] to produce two different mouse strains with the same *Srr2* deletion, in order to discriminate between the effects of the desired mutation, which would be common to both guides, and potential off-target effects of the guides which would be in contrast specific to a particular pair. Founders were genotyped for SRR2 deletion by PCR and mosaicism estimated using the MiSeq system (Illumina) (Table S3, adaptor sequence in bold). Two founders were chosen to establish two independent strains.

Immunofluorescence, EdU staining, image acquisition and pre-processing

Immunofluorescence was performed as previously described [64]. Mice were perfused with 4% w/v paraformaldehyde in phosphate-buffered saline (PBS), pituitaries harvested and cryosectioned at 12 µm. Sections were blocked with blocking solution (10% v/v donkey serum in PBS/0.1% v/v Triton X-100; PBST) for 1 hr, then incubated with primary antibodies in 10% blocking solution overnight at 4°C. Primary antibodies were used at the following dilutions: rat anti-GFP (Nacalai Tesque) at 1:1000; rabbit anti-POMC (NHPP) at 1:500; mouse anti-POMC [65] 1:500, Mouse anti-PAX7 (DSHB) 1:100, goat anti-SOX2 (Immune System) at 1:300, rabbit anti-SOX9 (gift from F. Poulat, Institut de Génétique Humaine, Montpellier) at 1:300, rat anti-CD31 [66] 1:50, p27kip C19 (SantaCruz) 1:300, rabbit anti-ki67 (Abcam) 1:1000. Sections were washed in PBST then incubated for 1 hr at room temperature with the corresponding anti-rat, anti-goat or anti-rabbit secondary antibody conjugated to Alexa-Fluor 488, 555, 594 or 647 in 10% blocking solution with 1 µM 4',6-diamino-2-phenylindole (DAPI).

Cell proliferation was analysed following a one-hour EdU pulse in E18.5 embryos (30µg/g body weight), or two intraperitoneal daily injections for 3 consecutive days in adult. Adult pituitaries were harvested at day 4. EdU incorporation was detected using the Click-iT EdU imaging kit following the manufacturer instructions (Thermo Fisher Scientific). Sections were washed with PBST and mounted using Aqua-Poly/Mount (Polysciences, Inc., Warrington, PA, USA).
Images were acquired using a Leica SPE confocal microscope or Olympus VS120 Slide Scanner. Settings were established during the initial acquisition. All images taken from the Leica SPE confocal microscope were pre-processed using ImageJ (maximum z-projection) and the ones taken from VS120 Slide Scanner were processed using Qu-path.

Immunohistochemistry

Pituitary glands were fixed in 10% buffered formaldehyde for 16 hours and embedded in paraffin. For staining, 4µm sections were de-paraffinized using xylene and rehydrated through a graded series of ethanol. Antigen retrieval was performed for 20 min at high temperature in either 0.01M citrate buffer (pH6) or Tris-EDTA (10mM Tris base, 1mM EDTA solution, pH9), depending on the antibody. The following antibodies were used: Sox2 (AF2018, R&D), 1:100, on sections treated with antigen retrieval buffer (Ventana) for 48 minutes, followed by a one hour primary antibody incubation. IHC was performed on the Discovery Ultra Ventana platform (Roche). P-ERK1/2 (4370, Cell Signalling Technology) 1:100 O/N at 4ºC, antigen retrieval was performed in the microwave for 23 minutes with 0.01M citrate buffer pH6. Goat anti-rabbit secondary antibody (BA-1000, Vector) was incubated 1:250 for 45 minutes at RT and then signal amplification and HRP detection were performed using the ABC kit (Vectorlabs) for 30 minutes at RT. This IHC was performed manually. Samples were blocked using 1% BSA and incubated overnight at 4°C with the desired antibody, or in blocking buffer for controls. Finally, slides were incubated with the secondary antibody for one hour and washed three times with PBS. For colorimetric staining with diaminobenzidine (DAB) slides were incubated with peroxidase substrate and mounted.

Cell Countings

For proliferation assays quantification, three different fields were chosen on different sections (sections always include IL, SCs flanking the cleft and AL). Within these, the numbers of SOX2-positive, SOX9-positive, EdU-positive, and SOX2;EdU;SOX9 triple-positive cells, representing proliferative stem cells, or SOX9 negative, SOX2;EdU double-positive cells, representing proliferative melanotrophs, were counted blindly and manually.
In EdU injected *Pomc-CreERT2; Sox2*$^{fl/+}$*;p27*$^{-/-}$*;Rosa26*$^{ReYFP/+}$ mutants, a total of around 1000 PAX7 positive cells was counted from fields randomly chosen and encompassing the whole IL. The number of EdU;PAX7-double-positive or EdU;PAX7;eYFP-triple-positive cells was counted blindly and manually, and the IL surface area was determined using the Fiji software.
The Fiji software was used to pseudocolor the different channels in unprocessed micrographs.
The Qupath software [67] was also used for image analysis. Briefly, areas of interest were defined after POMC immunostaining for the intermediate lobe, or SOX2;SOX9 for the SC layer. Within the areas of interest, the centre of cell nuclei was then identified as maxima in a filtered DAPI image. Nuclear boundaries were assigned by a propagation algorithm, and then expanded by ~1 micron to define sampling areas. The following data were then recorded: (i) average pixel intensities for each data channel over each sampling area, representing one cell, (ii) the size of the sampling areas; and (iii) the number of positive cells for each data channel over each sampling area.

Pituitary Dissociation for FACS, sc-RNAseq and Sphere Assay

Pituitaries were harvested, the posterior lobe was removed and the anterior and intermediate lobes isolated and incubated separately in a solution of papain (10108014001, Sigma-Aldrich, 1mg/ml in HBSS) for 15 min at 37ºC in presence of 10□g/ml of both DNAse (10104159001, Thermo Scientific) and Rock Inhibitor (M1817, Abmole Bioscience). The papain solution was then removed, and mechanical dissociation was performed on ice in pituisphere medium [27]. Pituispheres were derived as previously described [27] and spheres counted manually and blindly after 1 week in culture.

mRNA extraction and reverse transcriptase-PCR (rt-qPCR)

Total mRNA was extracted from dissected IL using the RNeasy Micro kit (Qiagen) according to the manufacturer's protocol. The extracted RNA was reverse-transcribed into cDNA using the Superscript VILO cDNA synthesis kit (Thermo Fisher Scientific, Figure 2) or SMART-Seq v4 Ultra Low Input RNA Kit (Takara Bio USA, Figure 5) according to the manufacturer's protocol.

Quantitative real-time PCR (RT-qPCR)

Each sample was assayed in technical duplicate with each tube containing diluted template cDNA, 250 nM primers and 1xAbsoluteSybrGreen ROX mix (Thermo Fisher Scientific). Each sample was assayed for the genes of interest together with the reference housekeeping gene *Gapdh* (Table S4). Relative expression of the genes of interest was calculated by normalisation of the detected expression value to the geometric mean of the reference genes using the ΔΔCt method [68]. Data is shown as mean±SEM with the number of biological samples indicated in each figure. Sidak's (Figure 1I) and Tukey's multiple comparison tests (Figure 2H and 5K) were used to assess significance of the data.

Radioimmunoassay (RIA)

Pituitaries were homogenized in phosphate-buffered saline and hormonal contents measured by RIA [69] using National Hormone and Pituitary Program reagents kindly provided by A.L. Parlow for ACTH and GH and using alpha MSH RIA kit (RB303-Invitech).

In-situ hybridization (RNAscope)

Fluorescent in situ hybridisations were performed manually using RNAscope (Multiplex Fluorescent Reagent Kit v2, 320293) on cryosections according to the manufacturer's protocol. Images were analysed and quantified using the Fiji package.

Statistical analyses

Statistical analyses were performed using Prism v.8.0c (GraphPad Software, USA). To examine significance of the data, tests were selected according to the experiment analysed. For survival curves generated using the Kaplan Meier method, log-rank tests were applied (Fig.2B). When comparing two groups of values with normal distribution, unpaired t-test was performed (Figure; 1H, 3H, 3I and in Supplementary figure;1B & 4B). Angular transformation was applied to compare percentages followed by unpaired t-test (Figure; 1L,1M, 2E and 3D. When comparing two groups of values where the distribution was non-parametric, Mann Whitney test was performed (Figure; 1C (upper graph), 1G, 1J). For multiple comparisons, analysis of variance (ANOVA) was implemented; Sidak's test was performed when comparing two groups (genotype) and differences between compartments (AL, SC cleft or IL) in Figure; 1C (bottom panel),1K,1O. To analyse larger groups, Tukey's multiple comparison test was implemented (Figure 2G, 2M & O, 3C,3K,4C,4D,4E and Supplementary

Figure;2B,4A). All results are represented as means ± standard deviation (SD) for raw data and means ± standard error of the mean (SEM) for graphs. Standard significance levels were used: *p<0.05, **p<0.01, ***p<0.001, ****p<0.0001.

RNA sequencing sample preparation

Bulk RNA sequencing. RNA was extracted from dissected male and female IL or FAC sorted cells using the RNeasy Micro kit (Qiagen) according to the manufacturer's protocol. RNA quality was assessed using the Agilent RNA 6000 Pico Kit (Agilent Technologies). cDNA was generated using Ovation RNA-seq System V2 (Tecan, 7102-A01), libraries were constructed using Ovation Ultralow System V2 (Tecan, 0344NB-A01) according to the manufacturer's instructions. Libraries were quantified using the TapeStation (Agilent) and pooled in equimolar proportions. Library were sequenced on an Hiseq4000 (Illumina), to achieve an average of 25 million reads per sample.

Single-cell RNA sequencing. Male and female IL cells were dissociated as described above. Libraries were generated using Chromium Single Cell 3' kit v3 (10x genomics, 100092) according to the manufacturer's instructions. Both cDNA and libraries were quantified using the TapeStation (Agilent) and sequenced on an Hiseq4000 (Illumina), to achieve an average of 50,000 reads per cell.

Bioinformatics analysis

Bulk RNA sequencing. The sequencing was performed on biological duplicates or triplicates for each data point. The RSEM package (version 1.3.30) [70] was used in conjunction with the STAR alignment algorithm (version 2.5.2a) [71] for the mapping and subsequent gene-level counting of the sequenced reads with respect to Ensembl mouse GRCm.38.89 version transcriptome. All parameters for RSEM were run as default except "–forward-prob" which was set to 0.5. Normalisation of raw count data and differential expression analysis was performed with the DESeq2 package (version 1.18.1) [72] within the R programming environment (version 3.4.3) [73]. Differentially expressed genes were defined as those showing statistically significant differences between pairwise groups if the adjusted P value was less than 0.05 (FDR < 0.05). Differentially expressed genes were taken forward and their pathway and process enrichments were analysed using Metacore (https://portal.genego.com). A hypergeometric test was used to determine statistical enriched pathways and processes and the associated P-value was corrected using the Benjamini–Hochberg method.

Single-cell RNA sequencing. 10x CellRanger (version.3.0.2) was used to generate single cell count data for each genotype (*Sox9*$^{iCreERT2/+}$*;Rosa26*$^{ReYFP/+}$, *Sox9*$^{iCreERT2/+}$*;p27*$^{-/-}$ *Rosa26*$^{ReYFP/+}$ and *Sox9*$^{iCreERT2/+}$*;Sox2*$^{fl/+}$*;p27*$^{-/-}$ *Rosa26*$^{ReYFP/+}$) using a transcriptome built from the Ensembl mouse GRCm38 release 89. All subsequent analyses were performed in R v.3.6.0 using the Seurat (v3) package [74]. Primary filtering was performed on each dataset by removing from consideration: cells expressing fewer than 50 genes and cells for which mitochondrial genes made up greater than 10% of all expressed genes. Each dataset was normalised using the' LogNormalize' function, with a scale factor of 10,000. The top 2000 highly variable genes were found using the 'FindVariableGenes' function and the data centred and scaled using the 'ScaleData' function. PCA decomposition was performed and after consideration of the eigenvalue 'elbow-plots, the first 20 components were used to construct Uniform Manifold Approximation Projection (UMAP) plots. Clusters relating to Melanotrophs and Stem Cells were identified, using the expression of known markers [melanotroph markers : Pomc, Pax7 and Pcsk2; stem cell markers : Sox2 and Sox9], and these clusters were integrated across the three genotypes (*Sox9*$^{iCreERT2/+}$*;Rosa26*$^{ReYFP/+}$, *Sox9*$^{iCreERT2/+}$*;p27*$^{-/-}$ *Rosa26*$^{ReYFP/+}$ and *Sox9*$^{iCreERT2/+}$*;Sox2*$^{fl/+}$*;p27*$^{-/-}$ *Rosa26*$^{ReYFP/+}$) using Seurat 3's standard integration

workflow. Differentially expressed genes between clusters across genotypes were determined using the 'FindMarkers" function.

Data availability

The RNA-sequencing datasets have been deposited in the Gene Expression Omnibus with the grouped accession number GSE152010. The bulk RNAseq datasets are GSE152007 (*p27*$^{-/-}$ IL compared to wild-type, two- and seven-month old) and GSE152008 (*p27*$^{-/-}$ IL compared to *p27*$^{-/-}$*;Sox2*$^{+/-}$ and wild-type, two- to three-month old); the single-cell RNA-sequencing datasets have been deposited with accession number GSE152009.

Figure legends

Figure 1. The expression of stem cell and differentiation markers is affected in *p27* -/- IL.

A) Double immunofluorescence for p27 and SOX2 in wild-type and *p27*-/- adult pituitaries. p27 is expressed at high levels in AL and in SCs lining the cleft, but at low levels in melanotrophs. SOX2 is expressed at high levels in SCs and low levels in melanotrophs of control pituitaries. In *p27*-/- IL, SOX2 staining is more intense in both cell types.
B) *In situ* hybridisation for *Sox2* in a 2-month old pituitary. In *p27*-/- IL higher levels of *Sox2* are observed in both melanotrophs and SCs .
C) Quantification of SOX2/*Sox2* expression levels in *p27*-/- versus wild-type.
Levels of expression were quantified after immunofluorescence in melanotrophs (A, left graph) and after *in situ* hybridisation, in the cell types indicated (B, right graph). In melanotrophs, the ratio between staining intensity in SOX2+melanotroph/SOX2+ SC in AL parenchyma is represented. In WT, SOX2 staining in melanotrophs is less intense than in AL SCs (0.63±0.20) while in *p27*-/- it becomes similar (0.91±0.16); (*p=0.019, n=4-6 in each group). Quantification after RNAscope show that in *p27*-/- , SCs flanking the cleft express *Sox2* at higher levels (28±6) than and wt (11.4±8, ***p=0.0002). The same is observed in melanotrophs: *p27*-/- (12±2) and wt (3.5±2.5, *p=0.0134), (n=5-4 in each group).
D-E) Bulk RNAseq pathway analysis in 2 month-old IL before tumor formation (*p27*-/- n=2 vs wt n=3, adjusted p-value <0.05) (**D**), and in 7 month-old hyperplastic IL (*p27*-/- n=4 vs wt n=2) (**E**).
F) Heatmap of representative genes expression from affected pathways shown in **D** and **E**.
G) POMC immunofluorescence in control and *p27*-/- adult pituitaries. POMC staining appears reduced in mutant melanotrophs (IL), while corticotroph levels in AL appear normal. The graphs represent quantification of POMC intensity in melanotrophs in relation to corticotrophs at e18.5 in wt (1.01±0.17, n=5) and *p27*-/- (1.10±0.19, n=5) and in 2 to 4 month-old animals, where levels are significantly reduced in mutants (wt:2.42±0.76, n=3; *p27*-/-:1.1±0.07, n=4, *p=0.0286).
H) MSH and ACTH contents were measured by RIA in 2 month-old pituitaries. *p27*-/- pituitaries contain less MSH (*p=0.0306, n=4 in each group) while there is no significant difference in ACTH levels (bottom graph).
I) Quantitative analysis of melanotroph marker expression levels by RT-qPCR in 2 to 3 month-old *p27*-/- and wt. *Pomc* (wt:1.03±0.27, n=3; *p27*-/-:0.32±0.09, n=3,**p=0.0013) and *T-pit* levels (wt:0.94±0.08, n=3; *p27*-/-:0.30±0.10, n=3,**p=0.0071) were reduced in mutants. *Pax7* levels appeared similarly affected but this did not reach statistical significance (wt:0.84±0.19, n=3; *p27*-/- :0.5±0.15, n=2).
J) Average cell size of melanotrophs. *p27*-/- melanotrophs (99±5.6, n=5) are smaller compared to wt (132±10, n=3,***p=0.0007).
K-N) Analysis of cell proliferation. EdU incorporation was quantified in melanotrophs, (SOX2;PAX7 double positive in K or SOX2 positive;SOX9 negative positive cells in L and M) and SCs (SOX2 positive;PAX7 negative cells in K or SOX2;SOX9 double positive in L and M). SCs were further distinguished as ventral or dorsal according to their localisation in the epithelial layer flanking the anterior or intermediate lobe respectively. At e18.5 (**K**) proliferation is not significantly different between mutants and controls (n=5), but there is a tendency toward more proliferation in mutant melanotrophs. In 1 month-old mice (**L**) , there is a significant increase in cell proliferation in both *p27*-/- melanotrophs and dorsal cleft SCs (n = 3 to 4 mice/genotype, melanotrophs *p=0.0235, dorsal cleft *p=0.0419). In 7 month-old mice, (**M**) cell proliferation is increased in melanotrophs and

both dorsal and ventral cleft SCs (n = 3 mice /genotype, melanotrophs *p=0.0167, dorsal cleft **p=0.0085, ventral cleft *p=0.0229).
N) SOX2, SOX9 and EdU triple staining in 1-month old wt and *p27-/-* animals.
O) Immunofluorescence for SOX2 on pituispheres obtained from IL wt and *p27-/-* 2 to 3 month-old animals. The proportion of pituispheres is increased in mutant IL (***p<0.0001, n=6-8 in each group).
P) Immunofluorescence for CD31 in 1-month old control and *p27-/-* pituitaries. In control pituitaries IL is avascular while *p27-/-* ILs show ectopic blood vessels at early stages (arrows).
Scale bars represent 20µm for A and N and O, 30µm for B, 50µm for G, 100µm for P. Cleft is outlined in A, B, N and P, IL is outlined G, N.

Figure2. Deletion of one copy of *Sox2* or of its enhancer Srr2 in *p27-/-* animals results in reduction of cell proliferation and impairment of tumorigenesis.

A) Brightfield pictures of wt, *Sox2+/-, p27-/- and p27-/-;Sox2+/-* pituitaries. In *p27-/-;Sox2+/-*IL tumourigenesis is impaired, but hyperplasia is observed.
B) Kaplan-Meier survival curves for wt, *Sox2+/-, p27-/-* and *p27-/-; Sox2+/-* animals. *p27-/-; Sox2+/-* mutants survive longer (17.1 months, n=10) than *p27-/-* mutants (12.5 months, n=28, *p<0.01), but still significantly less than wt (27 months, n=14,****p<0.0001).
C) Tumour incidence in the most affected organs in *p27-/-* mice. *Sox2* heterozygosity results in a reduction of tumour incidence in the pituitary and duodenum but not in lungs.
D) Comparison modalities for RNA-seq analysis of wild-type, *p27-/-* and *p27-/-;Sox2+/-* 2 to 3 month-old IL samples (wt n=4, *p27-/-* n=3, *p27-/-;Sox2+/-* n=3, adjusted p-value <0.05) (left panel). Enriched pathways are represented (centre panel) and heatmap of representative genes expression from affected pathways (right panel).
E) Analysis of cell proliferation. EdU incorporation was quantified in melanotrophs (SOX2 positive;SOX9 negative cells) and SCs (SOX2;SOX9 double positive cells). SCs were further distinguished as ventral or dorsal according to their localisation in the epithelial layer flanking the anterior or intermediate lobe respectively. Deletion of one copy of *Sox2* in compound mutants results in a reduction of cell proliferation compared to *p27-/-* samples in dorsal cleft SCs (n = 3-4 mice/genotype, *p=0.0208), melanotrophs.
F) SOX2 and EdU double staining in 2- to 3-month old wt, *p27-/-* and *p27-/-;Sox2+/-* animals. There is a clear reduction in SOX2 levels in *p27-/-;Sox2+/-* IL.
G) Proportion of pituispheres obtained from AL and IL wt, *Sox2+/-, p27-/- and p27-/-;Sox2+/-,* 2- to 3-month old animals. There is a reduction in the proportion of pituispheres formed from *p27-/-;Sox2+/-* IL compared to *p27-/-* samples, with the proportion in double mutants resembling that of wild type. wt (1±0.11,n=5), *Sox2+/-*(0.2±0.08,n=2), *p27-/-*(2.09±0.31,n=4) and *p27-/-;Sox2+/-*(1±0.52,n=3), ****p<0.0001 and ***p=0.0002; the reduction in *Sox2+/-* samples in agreement with the slightly hypomorphic pituitaries observed in *Sox2* heterozygous mice [38] and with SOX2 being required for proliferation of pituitary progenitors in the embryo [26 39].
H) Quantitative analysis of melanotroph marker expression levels by RT-qPCR in 2- to 3-month old wt, *Sox2+/-*, *p27-/-* and *p27-/- ;Sox2+/-* IL. In *p27-/-;Sox2+/-* animals, *Tbx19* expression levels are restored to wt levels. *Pomc*; wt (n=3) vs *p27-/-;Sox2+/-* (n=3), *p=0.03 and wt vs *p27-/-*(n=3), **p=0.0022, *Tbx19*; wt vs *p27-/-;Sox2+/-* (n=3, p=ns) and wt vs *p27-/-* (n=3,*p=0.0169).
I) Schematic representation of the *Sox2* murine locus and *Srr2* deletions engineered by genome editing. Two pairs of sgRNA (pair 1: guide 1_5' and guide 1_3' and pair 2: guide 4_5' and guide

5_3', PAM sequence in orange) were designed for *Srr2* (green box) deletion. The primers used to genotype *Srr2* deleted animals are marked by red arrows. Three founders deleted for *Srr2* were used to generate stable lines (1 to 3); the size of the deletion is indicated for each line.

J) Gel electrophoresis showing mosaic loss of *Srr2* in founder mice generated with sgRNA pair 1 (guide 1/1) or 2 (guide 4/5). The number above each lane corresponds to a individual founders. Boxed numbers below indicate strain derived from that particular founder.

K) Brightfield pictures of wt, *Srr2*$_{del/del}$, *p27*$_{-/-}$ and *p27*$_{-/-}$*;Srr2*$_{del/del}$ pituitaries. Deletion of two copies of *Sox2* Srr2 on a *p27*$_{-/-}$ background is sufficient to delay tumorigenesis.

L) Histological sections of H&E stained retinas. In *p27*$_{-/-}$*;srr2*$_{del/del}$ retina, size and organization of the layers is improved compared to *p27*$_{-/-}$. ONL = outer nuclear layer; OPL= outer plexiform layer, INL = inner nuclear layer, IPL=inner plexiform layer, GCL= ganglion cell layer.

M) Analysis of cell proliferation. EdU incorporation was quantified in melanotrophs (SOX2+;SOX9-cells) and SCs (SOX2;SOX9 double positive cells) in 7-month old wt, *p27*$_{-/-}$ and *p27*$_{-/-}$*;Srr2*$_{del/del}$ animals. In *p27*$_{-/-}$*;Srr2*$_{del/del}$ animals, there is a reduction of proliferation in stem cells compared to *p27*$_{-/-}$ (*p27*$_{-/-}$ (12.33±5.37, n=4) vs *p27*$_{-/-}$*;Srr2*$_{del/del}$ (2.11±1.88,n=4), **p=0.0061), but not in melanotrophs (*p27*$_{-/-}$ (8.75±2.36) vs *p27*$_{-/-}$*;Srr2*$_{del/del}$ (6.45±4.01), p=ns).

N) SOX2 and EdU double staining in 7-month old *p27*$_{-/-}$ and *p27*$_{-/-}$*;Srr2*$_{del/del}$ animals. SOX2 expression appears decreased *in p27*$_{-/-}$*;Srr2*$_{del/del}$ IL.

Scale bars represent 100mm for A, 20µm for F and O, 1-0.6mm for L, 50µm for M. Cleft is underlined in F and O, IL is underlined in F wt panel.

O) Proportion of pituispheres obtained from IL in wt, *p27*$_{-/-}$ and *p27*$_{-/-}$*; Srr2*$_{del/del}$. The percentage of spheres formed from *p27*$_{-/-}$*; Srr2*$_{del/del}$ (0.02±0.007, n=3,p=ns) is not significantly higher than wt (0.006±0.005, n=3), in contrast with *p27*$_{-/-}$ samples (0.04±0.02, n=3, *p=0.0344) demonstrating that loss of *Srr2* has an impact on sphere forming efficiency in mutants.

Figure 3. Deletion of one copy of *Sox2* in *p27*$_{-/-}$ melanotrophs prevents IL tumorigenesis.

A) eYFP mosaic recombination pattern in 6-month old *Pomc-CreERT2;Rosa26R*$_{eYFP/+}$ and *Pomc-CreERT2;p27*$_{-/-}$*;Rosa26R*$_{eYFP/+}$ IL. Only a proportion of melanotrophs are eYFP positive after tamoxifen treatment.

B) SOX2 and EdU double staining in 6- to 8-month old *Pomc-CreERT2, Pomc-CreERT2;p27*$_{-/-}$ *and Pomc-CreERT2;Sox2*$_{fl/+}$*;p27*$_{-/-}$ pituitaries.

C) Analysis of cell proliferation. EdU incorporation was quantified in melanotrophs (SOX2+;POMC+cells). EdU levels are similarly elevated in both *p27*$_{-/-}$ samples. *Pomc-CreERT2;Sox2*$_{fl/+}$*;p27*$_{-/-}$ (7.53±2.92,n=4, **p=0.0023) and *Pomc-CreERT2;p27*$_{-/-}$ (7.68±1.20,n=8, ***p=0.0007) vs *Pomc-CreERT2* (controls), (1.60±0.55, n=3).

D-E) EdU incorporation was quantified in PAX7+ve;eYFP-ve (2.40±1.31, n=6) and in PAX7+ve;eYFP+ve double positive melanotrophs (0.78±0.86, n=6) in 2.5- to 6-month old *Pomc-CreERT2;Sox2*$_{fl/+}$*;p27*$_{-/-}$*;Rosa26*$_{ReYFP}$ mice, assuming that *Rosa26*$_{ReYFP}$ recombination reflects *Sox2* heterozygous deletion. In PAX7+ve;EYFP+ve double positive melanotrophs EdU incorporation is significantly reduced compared to PAX7+ve;eYFP-ve cells (*p=0.0210) demonstrating that loss of one copy of *Sox2* results in reduced proliferation in *p27*$_{-/-}$ melanotrophs.

E) EdU and eYFP and PAX7 triple staining. Most EdU;PAX7 positive cells (arrows) do not express eYFP in *Pomc-CreERT2;Sox2*$_{fl/+}$*;p27*$_{-/-}$*;Rosa26*$_{ReYFP}$ IL.

F) Brightfield pictures of *Pomc-Cre, Pomc-Cre;p27-/-* and *Pomc-Cre;Sox2fl/+;p27-/-* pituitaries. Deletion of one copy of *Sox2* using Pomc-Cre prevents IL tumorigenesis.
G) Double immunofluorescence for POMC and SOX9 in 6- to 10-month old animals illustrating reduced IL size in *Pomc-Cre;Sox2fl/+;p27-/-*.
H) Measurement of IL area in *Pomc-Cre;p27-/- (*1472054±808382, n=3) and Pomc-Cre;Sox2fl/+;p27-/- (495612±185861, n=3). IL area *in Pomc-Cre;Sox2fl/+;p27-/-* pituitaries represents a third of IL area in *p27-/-* mutants (**p=0.0041).
I) Quantification of POMC intensity in melanotrophs in relation to corticotrophs in 6- to 10-month old *Pomc-Cre;p27-/-* (1.13±0.11,n=3) vs *Pomc-Cre;Sox2fl/+;p27-/-* (1.89±0.29,n=3) animals, where levels are significantly increased, *p=0.0127.
J) *In situ* hybridisation for *Sox2* in 6.25- to 10-month old wild-type, *p27-/-*, *p27-/-;Sox2+/-* and *Pomc-Cre;Sox2fl/+;p27-/-* animals.
K) Quantification of *Sox2* levels following *in situ* hybridisation in AL, SC and IL. *Sox2* expression levels are reduced in both *p27-/-;Sox2+/-* and *Pomc-Cre;Sox2fl/+;p27-/-* melanotrophs and stem cells compared to *p27-/-* , showing respectively cell autonomous and paracrine effects following *Sox2* deletion in melanotrophs. Quantification of *Sox2* levels in melanotrophs: *p27-/-* (12.17±2.15,n=4), wt (3.5±2.5, **p<0.003), *p27-/-;Sox2+/-* (5.4±1, *p=0.0276), *Pomc-Cre;Sox2fl/+;p27-/-* (2.56±0.1, **p=0.0038). Quantification of *Sox2* levels in SCs: *p27-/-* (28±6,n=4), wt (11.4±8,n=5, ****p<0.0001), *p27-/-;Sox2+/-* (11.3±1.4,n=3, ****p<0.0001), *Pomc-Cre;Sox2fl/+;p27-/-* (19±3,n=3, **p=0.0039).
Scale bars represent 30 µm for A and J, 20 µm for E, 500 µm for B, F and G. IL is underlined A and B. IL and stem cell cleft underlined in I.IL=intermediate lobe and AL=anterior lobe.

Figure 4. SOX2 is required in SCs for tumorigenesis in *p27-/-* IL.

A) eYFP, SOX9 (middle panel) and eYFP, PAX7 (right panel) double stainings in 7- to 12-month old *Sox9iresCreERT2/+;Rosa26ReYFP/+* and *Sox9iresCreERT2/+;p27-/-;Rosa26ReYFP/+* animals. eYFP;SOX9 double positive cells are localized in the epithelium lining the cleft in both genotypes. Very few eYFP+, SOX9- and PAX7- cells are present in *Sox9iresCreERT2/+; Rosa26ReYFP/+* animals (arrows). In *Sox9iresCreERT2/+;p27-/- Rosa26ReYFP/+* pituitaries some rare eYFP;PAX7 double-positive cells are present, demonstrating low levels of differentiation into melanotroph (left panel).
B) Brightfield pictures (upper panel) and SOX2 immunohistochemistry (bottom panel) on sections of *Sox9iresCreERT2/+;Rosa26ReYFP/+*, *Sox9iresCreERT2/+;p27-/-* and *Sox9iresCreERT2/+;Sox2fl/+;p27-/-* pituitaries. In *Sox9iresCreERT2/+;Sox2fl/+;p27-/-* pituitaries tumorigenesis is impaired (one-year old 14% tumour incidence, n=7) compared to *Sox9iresCreERT2/+;p27-/-* (one-year old, n=5, 100% tumour incidence). The thickness of the SOX2 positive SC epithelium resembles that of control, demonstrating that reduction of *Sox2* dosage in SCs impairs *p27-/-* ILtumorigenesis.
C,D,F) Analysis of cell proliferation. EdU incorporation was quantified in SCs and melanotrophs in 7- to 12-month old *Sox9iresCreERT2/+*, *Sox9iresCreERT2/+;p27-/-* and *Sox9iresCreERT2/+;Sox2fl/+;p27-/-* IL.
C) In SCs (SOX2;SOX9 double-positive cells), there is a significant reduction of proliferation in *Sox9iresCreERT2/+;Sox2fl/+;p27-/-* samples (0.20±0.35, n=3, **p=0.0011) compared to *Sox9iresCreERT2/+;p27-/-* ones (3±0.68, n=3). In fact, proliferation in *Sox9iresCreERT2/+;Sox2fl/+;p27-/-* SC is similar to *Sox9iresCreERT2/+*controls (0.28±0.32,n=3, p=ns).
D) In melanotrophs (POMC+ cells), there is a reduction of cell proliferation in *Sox9iresCreERT2/+;Sox2fl/+;p27-/-* samples (1.88±0.72, n=6, **p=0.0033) compared to

Sox9$_{iresCreERT2/+}$*;p27*$_{-/-}$ (3.7±0.76 ,n=4); again proliferation in *Sox9*$_{iresCreERT2/+}$*;Sox2*$_{fl/+}$*;p27*$_{-/-}$ is similar to *Sox9*$_{iCreERT/+}$ controls (0.60±0.4,n=4, *p=0.03)

E) Quantification of the vascular structures ectopic development in 7- to 12-month old. *Sox9*$_{iresCreERT2/+}$, *Sox9*$_{iresCreERT2/+}$*;p27*$_{-/-}$ and *Sox9*$_{iresCreERT2/+}$*;Sox2*$_{fl/+}$*;p27*$_{-/-}$ animals. Deletion of one copy of *Sox2* in SC leads to a reduction in the development of ectopic blood vessels in IL.

IL vascular structures area: *Sox9*$_{iresCreERT2/+}$ (0.32±0.28, n=3), *Sox9*$_{iresCreERT2/+}$*;p27*$_{-/-}$ (2.56±1.26, n=3, (*p<0.03)) and *Sox9*$_{iresCreERT2/+}$*;Sox2*$_{fl/+}$*;p27*$_{-/-}$ (1.15±0.43, n=3).

F) EdU, SOX2 double staining in 7- to 12-month old *Sox9*$_{iresCreERT2/+}$, *Sox9*$_{iresCreERT2/+}$*;p27*$_{-/-}$ and *Sox9*$_{iresCreERT2/+}$*;Sox2*$_{fl/+}$*;p27*$_{-/-}$ pituitary glands. Right panel, immunofluorescence for CD31 showing ectopic blood vessel formation reduction in *Sox9*$_{iresCreERT2/+}$*;Sox2*$_{fl/+}$*;p27*$_{-/-}$sample.

Scale bars represent 30 µm for A, 20 µm for B (bottom panel), 500 µm for B (upper panel), F. IL is underlined F. Stem cell cleft underlined in A.IL=intermediate lobe and AL=anterior lobe.

Figure 5. Characterization of the transcriptomic effects of *Sox2* dosage reduction in SCs in *p27*$_{-/-}$ IL by single cell analysis.

A) UMAP (Uniform Manifold Approximation and Projection) visualization of 3 month-old *Sox9*$_{iresCreERT2/+}$ (n=2110 cells), *Sox9*$_{iresCreERT2/+}$ *;p27*$_{-/-}$ (n=4527 cells) and *Sox9*$_{iresCreERT2/+}$ *;Sox2*$_{fl/+}$*;p27*$_{-/-}$ (n=4305 cells) single cell RNAseq datasets from dissected ILs. Individual datasets were integrated on a unique UMAP plot from the three different genotypes (right panel).

B) Identification of clusters according to the expression of known markers. Melanotroph clusters, identified by the expression of *Pomc*, *Tbx19* and *Pax7* genes and non segregated in PCA, were merged in one single cluster.

C) Subclustering of the stem cell fraction (0.9 resolution) shows that segregation only partially correlates with genotype (right panel).

D) Representation of the proportion of cells of the indicated genotype in each cluster, *Sox9*$_{iresCreERT2/+}$ (n= 137 cells), *Sox9*$_{iresCreERT2/+}$ *;p27*$_{-/-}$ (n= 104 cells) and *Sox9*$_{iresCreERT2/+}$ *;Sox2*$_{fl/+}$*;p27*$_{-/-}$ (n= 82 cells).

E) Heatmap showing expression of 14 genes selected out of 36 differentially expressed genes (adjusted p-value <0.05) in *Sox9*$_{iresCreERT2/+}$ *;p27*$_{-/-}$ compared with *Sox9*$_{iresCreERT2/+}$ or *Sox9*$_{iresCreERT2/+}$ *;Sox2*$_{fl/+}$*;p27*$_{-/-}$.

F) Immunohistochemistry for p-ERK on *Sox9*$_{iresCreERT2/+}$, *Sox9*$_{iresCreERT2/+}$*;p27*$_{-/-}$ and *Sox9*$_{iresCreERT2/+}$*;Sox2*$_{fl/+}$*;p27*$_{-/-}$ pituitaries. While the MAPK/ERK pathway seems overactive in *p27*$_{-/-}$ SCs, p-ERK levels returns to normal levels upon deletion of one copy of *Sox2* in SCs.

G) Subclustering of the melanotroph fraction (0.2 resolution) shows that segregation correlates with genotype (right panel).

H) Representation of the proportion of cells of the indicated genotype in the most abundant cluster, *Sox9*$_{iresCreERT2/+}$ (n= 1272 cells), *Sox9*$_{iresCreERT2/+}$*;p27*$_{-/-}$ (n= 3561 cells) and *Sox9*$_{iresCreERT2/+}$ *;Sox2*$_{fl/+}$*;p27*$_{-/-}$ (n= 3006 cells).

I) Strategy followed for scRNA-seq analysis of *Sox9*$_{iresCreERT2/+}$*;p27*$_{-/-}$ vs *Sox9*$_{iresCreERT2/+}$ or/and *Sox9*$_{iresCreERT2/+}$*;Sox2*$_{fl/+}$*;p27*$_{-/-}$ melanotrophs.

J) Upper panel, pathway analysis on genes differentially expressed (adjusted p-value <0.05) in melanotrophs following the strategy delineated in (I). Pathways associated with secretory function and cytoskeleton are downregulated in *Sox9*$_{iresCreERT2/+}$*;p27*$_{-/-}$ cells. Bottom panel, process network analysis performed on genes differentially expressed between *Sox9*$_{iresCreERT2/+}$*;p27*$_{-/-}$ and *Sox9*$_{iresCreERT2/+}$*;Sox2*$_{fl/+}$*;p27*$_{-/-}$ melanotrophs (adjusted p-value <0.05). Processes associated with

translation and transcription are downregulated in *Sox9*$_{iresCreERT2/+}$*;p27*$_{-/-}$ melanotrophs, while genes promoting cell cycle progression are upregulated.
K) RT-qPCR analysis of *Tbx19* levels in 5 to 12 month-old *Sox9*$_{iresCreERT2/+}$, *Sox9*$_{iresCreERT2/+}$*;p27*$_{-/-}$, *Sox9*$_{iresCreERT2/+}$*;Sox2*$_{fl/+}$*;p27*$_{-/-}$ and *p27*$_{-/-}$*;Sox2*$_{+/-}$ IL. *Tbx19* levels are increased in *Sox9*$_{iresCreERT2/+}$*;Sox2*$_{fl/+}$*;p27*$_{-/-}$ (0.99±0.20, n=3, *p=0.02) and *p27*$_{-/-}$*;Sox2*$_{+/-}$(1.07±0.15, n=3, **p=0.0044) vs *Sox9*$_{iresCreERT2/+}$*;p27*$_{-/-}$ (0.58±0.28, n=4).

Supplementary figure 1: Analysis of *p27*$_{-/-}$ pituitaries.

A) Principal Component Analysis (PCA) plots of bulk RNA-seq data of 2- and 7-month old wildtype and *p27*$_{-/-}$ IL samples. There is a clear segregation of samples according to genotype, even before tumour formation (2 month-old). Furthermore while wild-type samples segregate according to age, *p27*$_{-/-}$ samples appear more similar, independently of the age of the animal.
B) GH content were measured by RIA in 2-month old male pituitaries. *p27*$_{-/-}$ pituitary glands contain higher GH levels (*p=0.0340, n=4 in each group) which is consistent with gigantism affecting these mutants.

Supplementary figure 2: Analysis of *p27*$_{-/-}$*;Sox2*$_{+/-}$ and *p27*$_{-/-}$*;Srr2*$_{del/del}$ pituitaries.

A) PCA plots of bulk RNA-seq data of 2- to 3-month old wild-type, *p27*$_{-/-}$ and *p27*$_{-/-}$*;Sox2*$_{+/-}$ ILs. *p27*$_{-/-}$*;Sox2*$_{+/-}$ samples are clustering between wild-type and *p27*$_{-/-}$ ones.
B) RT-qPCR analysis of *Sox2* in wild-type, *Sox2*$_{+/-}$, *p27*$_{-/-}$,and *p27*$_{-/-}$*;Sox2*$_{+/-}$ in 2- to 3-month old ILs. *Sox2* expression levels decrease in *Sox2*$_{+/-}$ and *Sox2*$_{+/-}$*;p27*$_{-/-}$ vs w*t or p27*$_{-/-}$. We did not observe an increase in *Sox2* levels in *p27*$_{-/-}$ using this technique. This may be because IL comprises two cell types expressing *Sox2* at different levels: a high proportion of melanotrophs, expressing it at low levels, and SCs, expressing it at high levels. In *p27*$_{-/-}$ animals there are many more melanotrophs than in wild-type, but these, despite *Sox2* derepression, are still expressing *Sox2* at lower levels than SCs (Fig.1A). The difference in proportion in both cell types between wildtype and mutant may explain the inability to observe *Sox2* derepression.
C) Genotypes of offspring obtained from *Srr2*$_{del/+}$ heterozygous (XX) and (XY) intercrosses.

Supplementary figure 3: Analysis of stem cells in *Sox9*$_{iresCreERT2/+}$*;Sox2*$_{fl/+}$*;p27*$_{-/-}$ pituitaries.

A) Analysis of tomato positive cells by flow cytometry in *Sox9*$_{iCreERT2/+}$*;Rosa26*$_{tdTomato/+}$, *Sox9*$_{iCreERT2/+}$*;p27*$_{-/-}$*;Rosa26*$_{tdTomato/+}$and *Sox9*$_{iCreERT2/+}$*;Sox2*$_{fl/+}$*;p27*$_{-/-}$*;Rosa26*$_{tdTomato/+}$ dissected IL from 3.5- to 5-month old animals that were treated by tamoxifen at 1month-old. The number of tomato-positive FACSorted stem cells is reduced in *Sox9*$_{iCreERT2/+}$*;Sox2*$_{fl/+}$*;p27*$_{-/-}$ *Rosa26*$_{tdTomato/+}$ (1953±1658, n=6) compared to *Sox9*$_{iCreERT2/+}$*;p27*$_{-/-}$*;Rosa26*$_{tdTomato/+}$ samples (4648±1954, n=7), to values comparable to control. (**p=0.0094 and *p=0.0189).
B) Quantification of SOX2 immunofluorescence intensity in the stem cell layer in *Sox9*$_{iCreERT2/+}$ (621±23 a.u, number of cells counted 1214, n=3 animals), *Sox9*$_{iCreERT2/+}$*;p27*$_{-/-}$ (1093±317 a.u, number of cells counted 899, n=3) and *Sox9*$_{iCreERT2/+}$*;Sox2*$_{fl/+}$*;p27*$_{-/-}$ (387±246 a.u, number of cells counted 1265, n=3) pituitaries of 7 to 12 month-old animals. *Sox9*$_{iCreERT2/+}$*;Sox2*$_{fl/+}$*;p27*$_{-/-}$ express lower levels of Sox2 (*p=0.02).

Supplementary Table 1: Genes differentially expressed in the SC clusters (Single-cell RNAseq analysis)

Genes differentially expressed in cluster 1 (comprising mostly *Sox9* $_{iresCreERT2/+}$*;p27*$_{-/-}$ cells*)* but unaffected in cluster 2 (comprising mostly *Sox9* $_{iresCreERT2/+}$*;p27*$_{-/-}$*;Sox2*$_{fl/+}$ cells) compared to cluster 0 (comprising mostly control *Sox9* $_{iresCreERT2/+}$ cells) are listed. The percentage of cells expressing the gene of interest in each cluster is represented, followed by the significance of differential expression versus control.

Supplementary figure 4: Model illustrating the effects of p27 on Srr2 enhancer and consequences of their loss in melanotrophs.

Srr2$_{del/del}$ animals do not phenocopy aspects of the *p27*$_{-/-}$ phenotype, which might have been expected if all the enhancer does is mediate repression of *Sox2* by P27. However, in agreement with the phenotype of *p27*$_{-/-}$*; Srr2*$_{del/del}$ animals, deletion of *Srr2* prevents both repression and derepression of SOX2. In *p27*$_{-/-}$*; Srr2*$_{del/del}$ animals we observe absence of both retinal defects and IL tumour formation. Therefore, the repressive action of P27 is mediated by *Srr2* and in absence of *p27*, *Srr2* activators drive *Sox2* expression leading to pituitary tumours and retina defects.

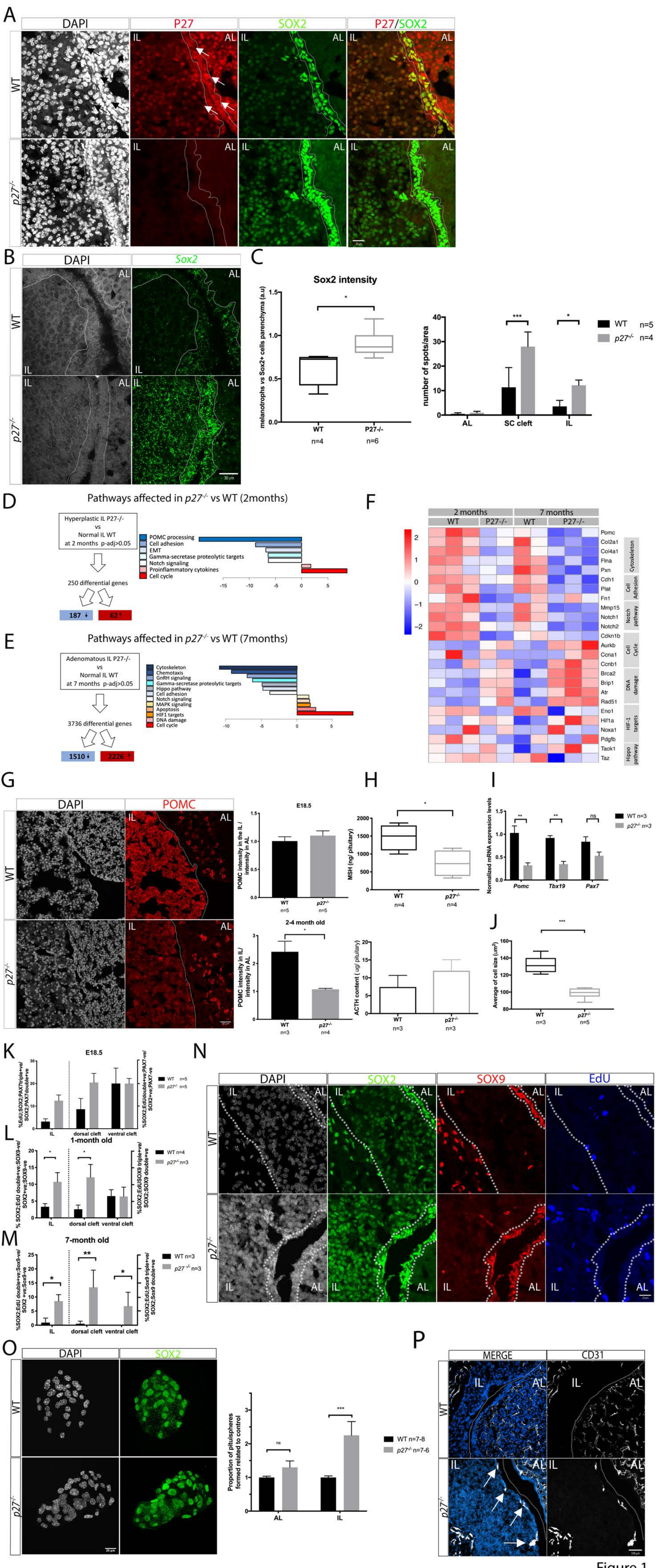
A
DAPI
P27
SOX2
P27/SOX2
WT
p27-/-
IL
AL
B
DAPI
Sox2
C
Sox2 intensity
melanotrophs vs Sox2+ cells parenchyma (a.u)
WT
P27-/-
n=4
n=6
number of spots/area
AL
SC cleft
IL
WT n=5
p27-/- n=4
D
Pathways affected in p27-/- vs WT (2months)
Hyperplastic IL P27-/- vs Normal IL WT at 2 months p-adj>0.05
250 differential genes
187
62
POMC processing
Cell adhesion
EMT
Gamma-secretase proteolytic targets
Notch signaling
Proinflammatory cytokines
Cell cycle
E
Pathways affected in p27-/- vs WT (7months)
Adenomatous IL P27-/- vs Normal IL WT at 7 months p-adj>0.05
3736 differential genes
1510
2226
Cytoskeleton
Chemotaxis
GnRH signaling
Gamma-secretase proteolytic targets
Hippo pathway
Cell adhesion
Notch signaling
MAPK signaling
Apoptosis
HIF1 targets
DNA damage
Cell cycle
F
2 months
7 months
WT
P27-/-
Pomc
Col2a1
Col4a1
Flna
Pxn
Cdh1
Plat
Fn1
Mmp15
Notch1
Notch2
Cdkn1b
Aurkb
Ccna1
Ccnb1
Brca2
Brip1
Atr
Rad51
Eno1
Hif1a
Noxa1
Pdgfb
Taok1
Taz
Cytoskeleton
Cell Adhesion
Notch pathway
Cell Cycle
DNA damage
HIF-1 targets
Hippo pathway
G
DAPI
POMC
E18.5
2-4 month old
POMC intensity in the IL / intensity in AL
H
MSH (ng/ pituitary)
ACTH content (ug/ pituitary)
I
Normalized mRNA expression levels
Pomc
Tbx19
Pax7
WT n=3
p27-/- n=3
J
Average of cell size (um²)
K
E18.5
%EdU;SOX2;PAX7triple+ve/ SOX2;PAX7double+ve
%SOX2;EdUdouble+ve;PAX7-ve/ SOX2+ve;PAX7-ve
IL
dorsal cleft
ventral cleft
WT n=5
p27-/- n=5
L
1-month old
% SOX2;EdU double+ve;SOX9-ve/ SOX2+ve;SOX9-ve
%SOX2;EdUSOX9 triple+ve/ SOX2;SOX9 double+ve
WT n=4
p27-/- n=3
M
7-month old
%SOX2;EdU double+ve;Sox9-ve/ SOX2 +ve;Sox9-ve
%SOX2;EdU;Sox9 triple+ve/ SOX2;Sox9 double+ve
WT n=3
p27-/- n=3
N
DAPI
SOX2
SOX9
EdU
O
DAPI
SOX2
Proportion of pituispheres formed related to control
ns
WT n=7-8
p27-/- n=7-6
P
MERGE
CD31

Figure 1

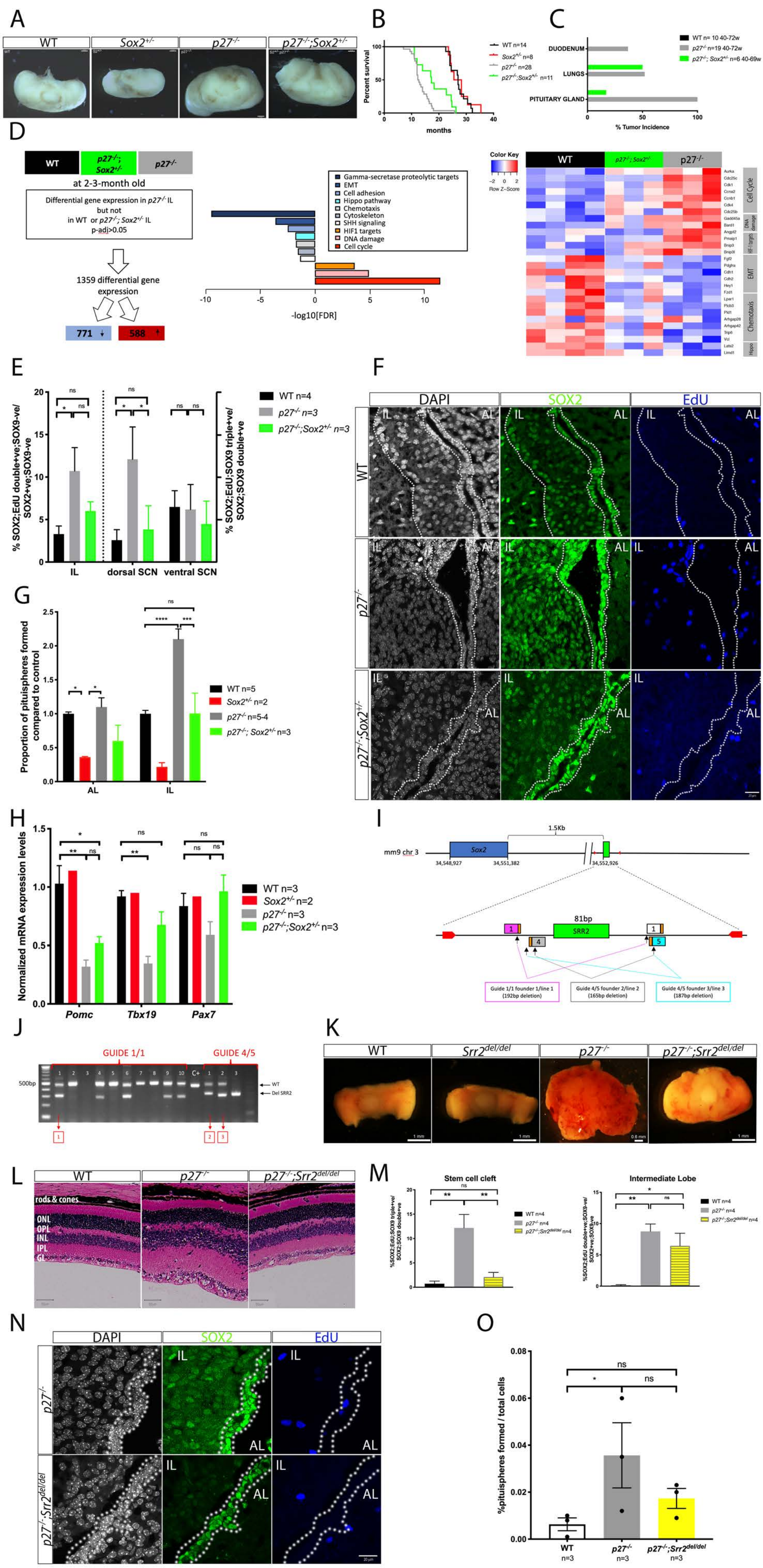
A
WT
Sox2+/-
p27-/-
p27-/-;Sox2+/-
B
Percent survival
months
WT n=14
Sox2+/- n=8
p27-/- n=28
p27-/-;Sox2+/- n=11
C
DUODENUM
LUNGS
PITUITARY GLAND
% Tumor Incidence
WT n= 10 40-72w
p27-/- n=19 40-72w
p27-/-; Sox2+/- n=6 40-69w
D
WT
p27-/-; Sox2+/-
p27-/-
at 2-3-month old
Differential gene expression in p27-/- IL but not in WT or p27-/-; Sox2+/- IL p-adj>0.05
1359 differential gene expression
771
588
Gamma-secretase proteolytic targets
EMT
Cell adhesion
Hippo pathway
Chemotaxis
Cytoskeleton
SHH signaling
HIF1 targets
DNA damage
Cell cycle
-log10[FDR]
Color Key
Row Z-Score
Cell Cycle
DNA damage
HIF-1 targets
EMT
Chemotaxis
Hippo
E
% SOX2;EdU double+ve;SOX9-ve/ SOX2+ve;SOX9-ve
% SOX2;EdU;SOX9 triple+ve/ SOX2;SOX9 double+ve
IL
dorsal SCN
ventral SCN
WT n=4
p27-/- n=3
p27-/-;Sox2+/- n=3
F
DAPI
SOX2
EdU
IL
AL
WT
p27-/-
p27-/-;Sox2+/-
G
Proportion of pituispheres formed compared to control
AL
IL
WT n=5
Sox2+/- n=2
p27-/- n=5-4
p27-/-; Sox2+/- n=3
H
Normalized mRNA expression levels
Pomc
Tbx19
Pax7
WT n=3
Sox2+/- n=2
p27-/- n=3
p27-/-;Sox2+/- n=3
I
1.5Kb
mm9 chr 3
Sox2
34,548,927
34,551,382
34,552,926
81bp
SRR2
Guide 1/1 founder 1/line 1 (192bp deletion)
Guide 4/5 founder 2/line 2 (165bp deletion)
Guide 4/5 founder 3/line 3 (187bp deletion)
J
GUIDE 1/1
GUIDE 4/5
500bp
WT
Del SRR2
K
WT
Srr2del/del
p27-/-
p27-/-;Srr2del/del
L
rods & cones
ONL
OPL
INL
IPL
GL
M
Stem cell cleft
Intermediate Lobe
WT n=4
p27-/- n=4
p27-/-;Srr2del/del n=4
N
DAPI
SOX2
EdU
O
%pituispheres formed / total cells
WT n=3
p27-/- n=3
p27-/-;Srr2del/del n=3

Figure 2

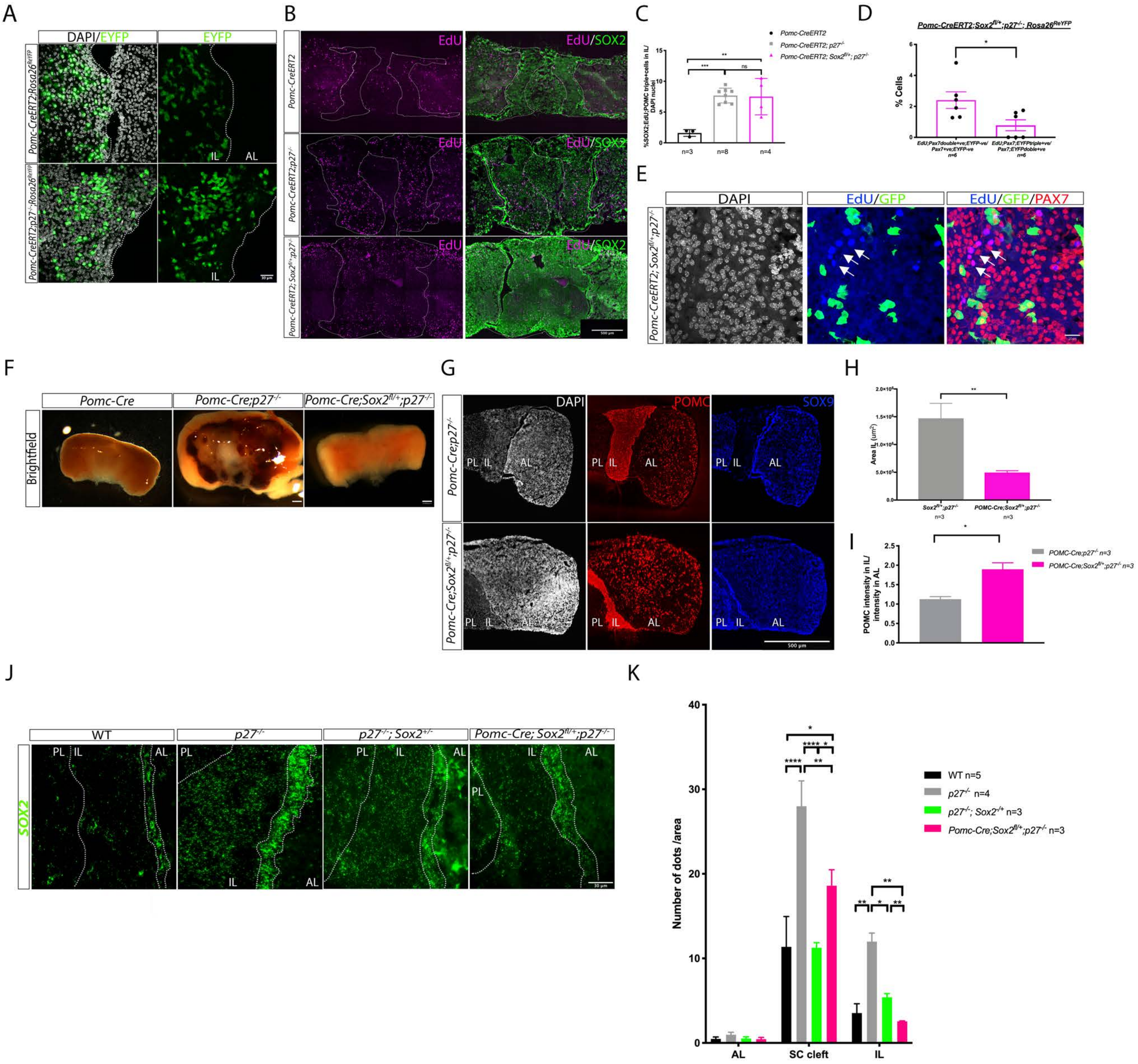
A
DAPI/EYFP
EYFP
Pomc-CreERT2;Rosa26ReYFP
Pomc-CreERT2;p27-/-;Rosa26ReYFP
IL
AL
B
EdU
EdU/SOX2
Pomc-CreERT2
Pomc-CreERT2;p27-/-
Pomc-CreERT2; Sox2fl/+;p27-/-
C
Pomc-CreERT2
Pomc-CreERT2; p27-/-
Pomc-CreERT2; Sox2fl/+; p27-/-
%SOX2;EdU;POMC triple+cells in IL/ DAPI nuclei
n=3
n=8
n=4
D
Pomc-CreERT2;Sox2fl/+;p27-/-; Rosa26ReYFP
% Cells
EdU;Pax7double+ve;EYFP-ve/ Pax7+ve;EYFP-ve n=6
EdU;Pax7;EYFPtriple+ve/ Pax7;EYFPdoble+ve n=6
E
DAPI
EdU/GFP
EdU/GFP/PAX7
Pomc-CreERT2; Sox2fl/+;p27-/-
F
Pomc-Cre
Pomc-Cre;p27-/-
Pomc-Cre;Sox2fl/+;p27-/-
Brightfield
G
DAPI
POMC
SOX9
Pomc-Cre;p27-/-
Pomc-Cre;Sox2fl/+;p27-/-
PL
IL
AL
H
Area IL (um2)
Sox2fl/+;p27-/-
POMC-Cre;Sox2fl/+;p27-/-
I
POMC intensity in IL/ intensity in AL
POMC-Cre;p27-/- n=3
POMC-Cre;Sox2fl/+;p27-/- n=3
J
WT
p27-/-
p27-/-; Sox2+/-
Pomc-Cre; Sox2fl/+;p27-/-
SOX2
K
Number of dots /area
WT n=5
p27-/- n=4
p27-/-; Sox2-/+ n=3
Pomc-Cre;Sox2fl/+;p27-/- n=3
AL
SC cleft
IL

Figure 3

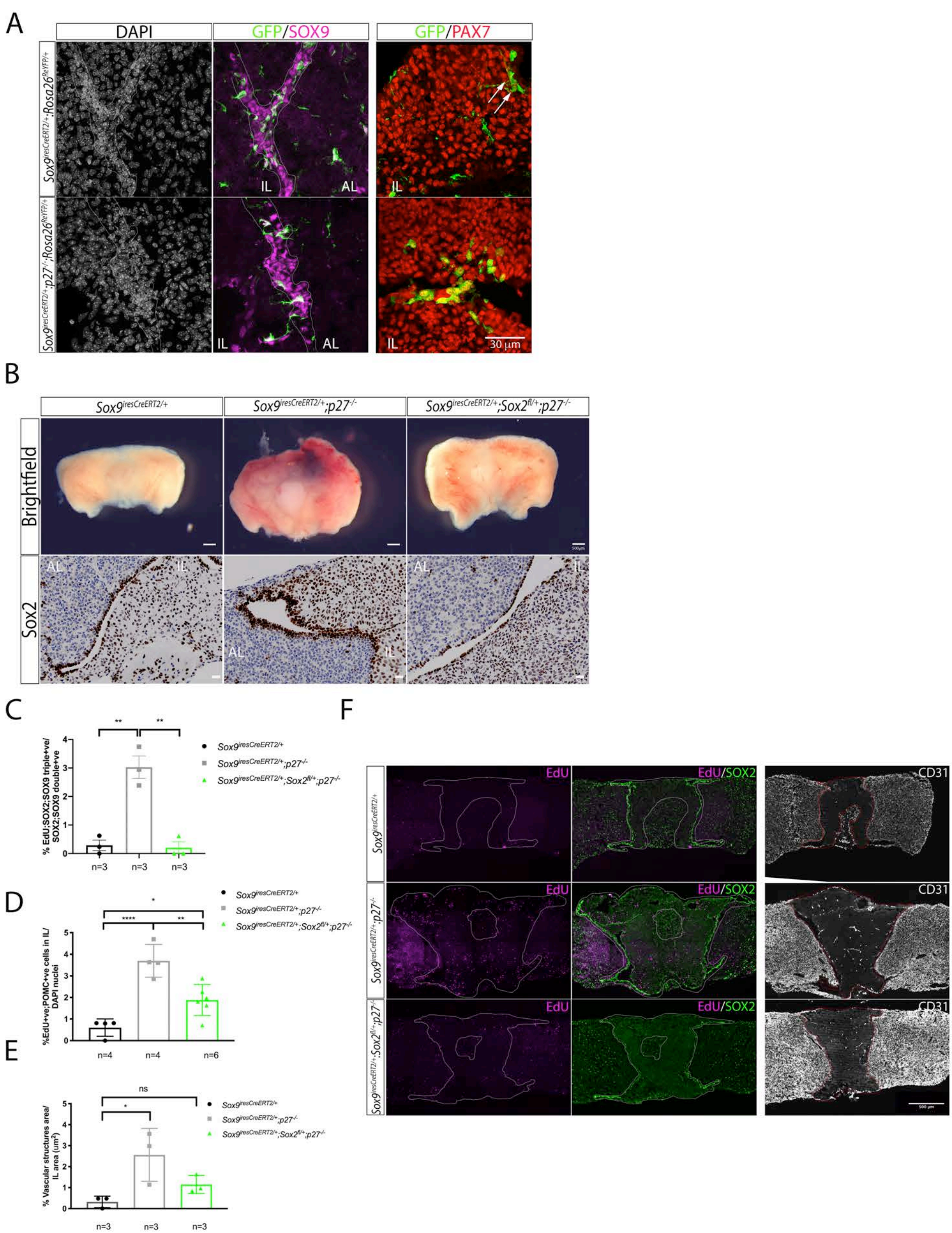
A
DAPI
GFP/SOX9
GFP/PAX7
Sox9iresCreERT2/+;Rosa26ReYFP/+
Sox9iresCreERT2/+;p27-/-;Rosa26ReYFP/+
IL
AL
30 µm
B
Sox9iresCreERT2/+
Sox9iresCreERT2/+;p27-/-
Sox9iresCreERT2/+;Sox2fl/+;p27-/-
Brightfield
Sox2
C
% EdU;SOX2;SOX9 triple+ve/ SOX2;SOX9 double+ve
n=3
n=3
n=3
D
%EdU+ve;POMC+ve cells in IL/ DAPI nuclei
n=4
n=4
n=6
E
% Vascular structures area/ IL area (um2)
ns
n=3
n=3
n=3
F
EdU
EdU/SOX2
CD31
500 µm

Figure 4

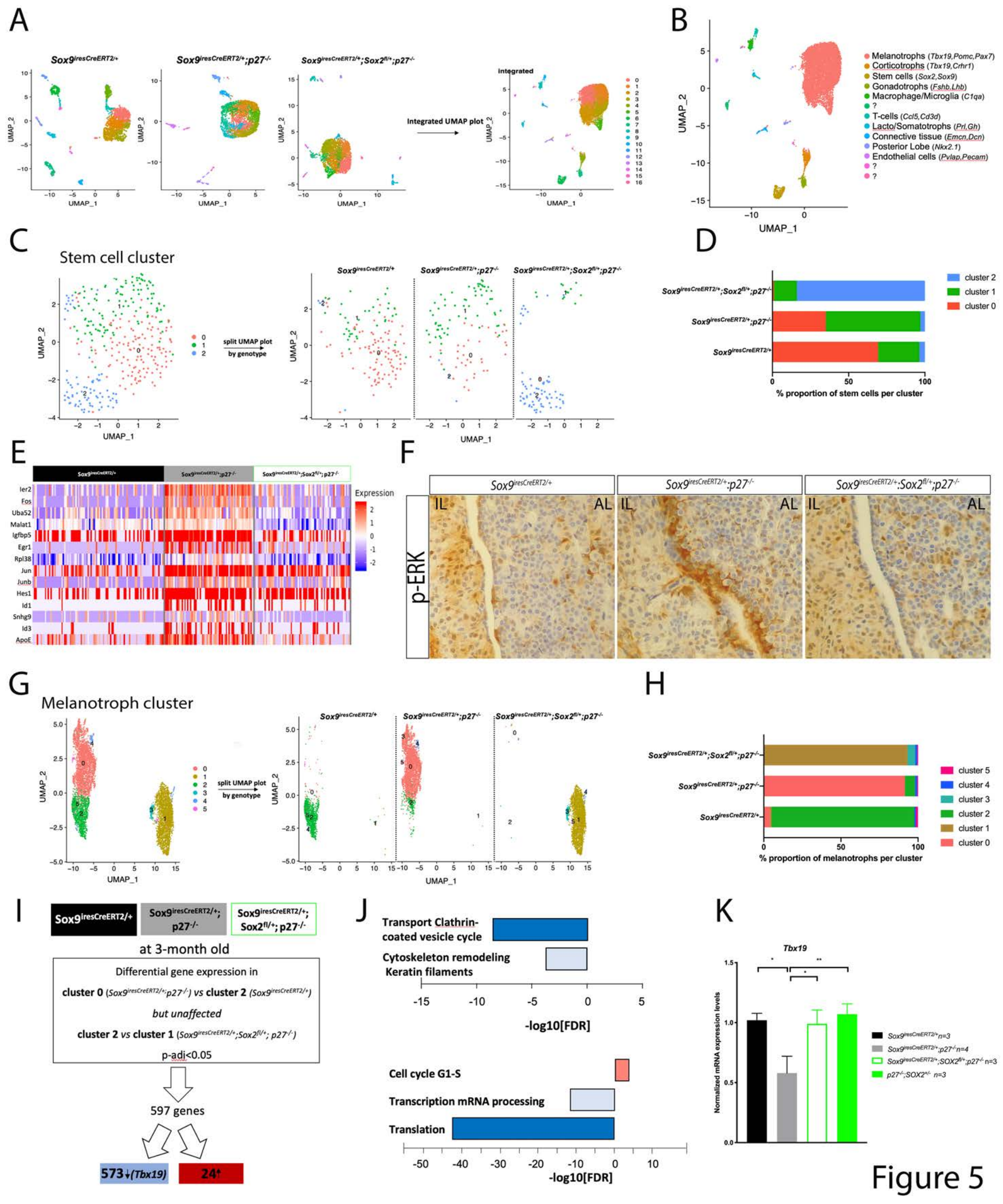
A
Sox9iresCreERT2/+
Sox9iresCreERT2/+;p27-/-
Sox9iresCreERT2/+;Sox2fl/+;p27-/-
Integrated
Integrated UMAP plot
UMAP_1
UMAP_2
B
Melanotrophs (Tbx19,Pomc,Pax7)
Corticotrophs (Tbx19,Crhr1)
Stem cells (Sox2,Sox9)
Gonadotrophs (Fshb,Lhb)
Macrophage/Microglia (C1qa)
?
T-cells (Ccl5,Cd3d)
Lacto/Somatotrophs (Prl,Gh)
Connective tissue (Emcn,Dcn)
Posterior Lobe (Nkx2.1)
Endothelial cells (Pvlap,Pecam)
?
?
C
Stem cell cluster
split UMAP plot by genotype
D
cluster 2
cluster 1
cluster 0
% proportion of stem cells per cluster
E
Expression
Ier2
Fos
Uba52
Malat1
Igfbp5
Egr1
Rpl38
Jun
Junb
Hes1
Id1
Snhg9
Id3
ApoE
F
p-ERK
IL
AL
G
Melanotroph cluster
split UMAP plot by genotype
H
cluster 5
cluster 4
cluster 3
cluster 2
cluster 1
cluster 0
% proportion of melanotrophs per cluster
I
Sox9iresCreERT2/+
Sox9iresCreERT2/+; p27-/-
Sox9iresCreERT2/+; Sox2fl/+; p27-/-
at 3-month old
Differential gene expression in
cluster 0 (Sox9iresCreERT2/+;p27-/-) vs cluster 2 (Sox9iresCreERT2/+)
but unaffected
cluster 2 vs cluster 1 (Sox9iresCreERT2/+;Sox2fl/+; p27-/-)
p-adj<0.05
597 genes
573↓(Tbx19)
24↑
J
Transport Clathrin-coated vesicle cycle
Cytoskeleton remodeling Keratin filaments
-log10[FDR]
Cell cycle G1-S
Transcription mRNA processing
Translation
-log10[FDR]
K
Tbx19
Normalized mRNA expression levels
Sox9iresCreERT2/+n=3
Sox9iresCreERT2/+;p27-/-n=4
Sox9iresCreERT2/+;SOX2fl/+;p27-/- n=3
p27-/-;SOX2+/- n=3

Figure 5